参赛队员姓名：　　杨佳炎

中学：　北京市十一学校

省份：　　北京市

国家/地区：　　　　　中国

指导教师姓名：　肖硕林，仲国虎

指导教师单位：美国康奈尔大学，

北京市十一学校

论文题目：

Alteration of Sediment Resuspension Threshold Condition Caused by Microplastic-Sediment Aggregation and Its Potential Influence on Climate Change

Alteration of Sediment Resuspension Threshold Condition Caused by Microplastic-Sediment Aggregation and Its Potential Influence on Climate Change

Jiayan Yang

September 2022

Abstract

Both plastic pollution and climate change are environmental problems worth addressing. This study focuses on how the two seemingly isolated issues may interact. The following hypothesis is proposed: A special kind of plastics, microplastics, may alter the threshold condition of sediment resuspension in rivers through forming aggregates with river sediments. Meanwhile, by releasing greenhouse gases located in the sediments, sediment resuspension may promote climate change. The study examines this hypothesis from three different perspectives: First, a theory explaining factors influencing sediment resuspension is built; Then, an experiment testing the formation of aggregates and the change of sediment resuspension critical shear velocity is conducted; Finally, the scenario is tested again using the method of computational fluid dynamics. The results suggest that the hypothesis is reasonable. By forming aggregates with sediments, microplastics reduces the overall density of the particles on riverbed and lowers the critical shear velocity of sediment resuspension, thus allowing more greenhouse gas emission. Under the conditions of this study, the overall density of the particles can be reduced to 1200 kg/m^3 from 2500 kg/m^3, and the critical shear velocity may decrease for about 14% to 25%.

Keywords: Microplastic Pollution, Sediment Resuspension, Climate Change, Microplastic-Sediment Aggregation, Critical Shear Velocity

Contents

1 Introduction

Environmental issues are receiving greater attention during the century as our society recognizes the impact of human activities on nature, as well as the reactions and threats conversely presented to humans by nature. However, despite the attention received, environmental issues can be complex to analyze and difficult to solve. The interactions between environment events are often understated, which may hinder our understanding of the existing problems, not mentioning solving these problems. In this research, one specific event of microplastic circulation, specifically the interaction between river sediment and microplastics, is investigated. Moreover, the potential impact of this event on the larger problem of climate change is discussed, which will shed light on how seemingly isolated environmental issues can intensify one another. A conceptional drawing of these events interacting with one another is shown in Figure 1.1.

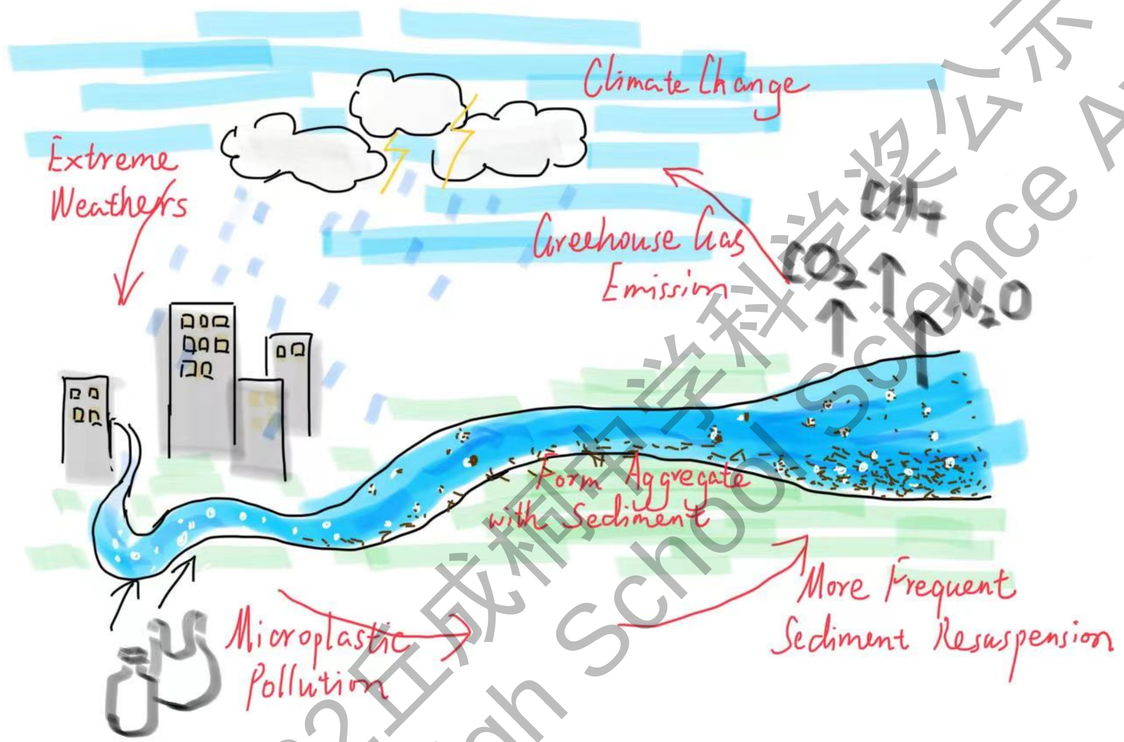

Figure 1.1: A conceptional drawing of the interactions between the three environmental events: Microplastic pollution, sediment resuspension, and climate change.

Microplastics are defined as plastics of size under 5mm. Microplastics have two main sources: primary or secondary. Primary microplastics are added to comestic products as abrasives. Secondary microplastics come from macroplastics that have broken into pieces, analogous to how sand form from stones. Due to their small size, microplastics are able to interact with the environment in new ways that macroplastics can not: Microplastics have a greater mobility as they can be driven by water and air. One pathway of microplastic circulation is to enter the river system. Wind or rain can easily transport microplastics concentrated in the cities into the river system. There, the microplastics are exposed to organisms and suspended particles in the water column. Microplastics can form aggregates with other sediment particles and sink down into the sediment. Notice, here aggregation doesn't mean microplastics and sediment particles are chemically bind, but physically attached due to electric forces, molecular forces, or stuck together by biofilms.

This aggregation process and the sedimentation process make microplastics incorporated into the river bed. The microplastic-sediment aggregates become part of the river sediment that is subject to the river events, primarily, the water's scouring. When the speed of the river reach a threshold, sediment particles may resuspend, being transported to the water column and move along the water. This process is called sediment resuspension. When microplastics-sediment aggregates exist in rivers, the properties of river beds may change. The sediments will have a lower overall density, for most microplastics has density around $1000kg/m^3$, smaller than the original river sediments. The sediment may also be more loosely packed, or become more rough on the surface. With these properties changed, the critical water speed for the sediment to resuspend may change.

If the critical condition of sediment resuspension may be altered by the formation of microplastic-sediment aggregates, how does sediment resuspension further connects to climate change? Rivers, like forests and oceans, are carbon reservoirs. Greenhouse gases, including CO_2, CH_4, and N_2O, are present in river sediments. These gases are produced by microorganisms in the rivers. As nutrients decay, greenhouse gases accumulates in the sediments. When sediments resuspend, large amounts of stored greenhouse gases are released into the water column, and may further reach the atmosphere. Therefore, if microplastics can change the critical shear velocity of sediment, it may influence the release of greenhouse gases. More specifically, if microplastics, after forming aggregates with river sediment, reduce the the critical shear stress of resuspension, more greenhouse gases will be released. Is there possibility that the three environmental events form a viscous cycle shown in Figure 1.2? This is the major question this study attempts to answer, or at least consider.

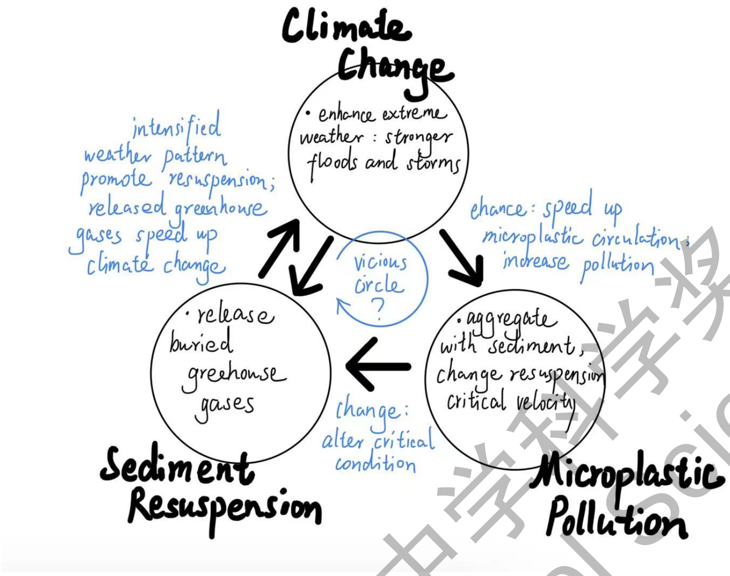

Figure 1.2: Will these environmental events form a vicious cycle?

2 Theory

The event that bridges microplastic pollution and greenhouse gas emission is sediment resuspension. The focus of this study is therefore the process of microplastic-sediment aggregates formation and their influence on sediment resuspension. The theory part will start with a force analysis of sediment resuspension, then moving to a well-accepted experiment based explanation of sediment resuspension. Finally, we will use the theory to discuss and predict how will microplastic, by forming aggregates with sediments, affect sediment resuspension.

2.1 Force Analysis: What Drives a Particle on River Bed?

Sediment is essentially made up by many small particles. Sediment resuspension is a state of motion of these particles. To understand sediment resuspension, we can start with analyzing the forces acting upon a particle submerged in moving water, located on the river bed. The particle is idealized to be of spherical shape.

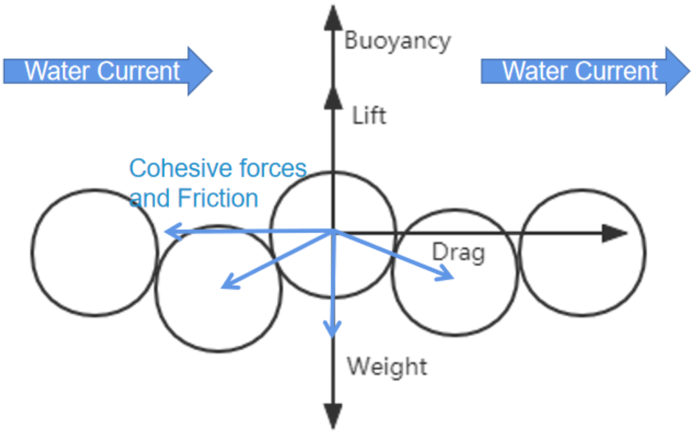

Figure 2.1: Forces at work during resuspension. Main forces are marked in black arrows. Blue arrows represent friction and cohesive forces that are of uncertain magnitudes and directions.

Figure 2.1 shows the forces at work during resuspension. We can divide them into two categories, the resisting forces and the promoting forces. Resisting forces refer to the forces that impedes the resuspension of the particle. Resisting forces include gravitational force, friction, and cohesive forces such as Van der Waals force and electrostatic force. Contrarily, promoting forces are the critical factors that contribute to the resuspension process. The change in magnitudes of these forces is the main reason of resuspension, as well as the focus of the study. Promoting forces include buoyancy, drag force, and lift force. Notice we ignore normal force. This is because when the particle is at the edge of resuspension, lift force and buoyancy balance with the weight, therefore there's no normal force anymore.

Now, we will give the formula of the main forces: Weight, Buoyancy, Lift, and Drag, to see the factors determining their magnitudes. Here, cohesive forces and friction are ignored because they are not the dominating factors influencing resuspension. Also, the magnitude and direction of cohesive forces depend on the angle of positioning of the particle among other particles, making cohesive forces and friction hard to describe.

$$F_G = \rho_s V g = \frac{1}{6}\pi\rho_s D^3 g \tag{1a}$$

$$F_B = \rho_w V g = \frac{1}{6}\pi\rho_w D^3 g \tag{1b}$$

where:
ρ_s : the density of the particle
ρ_w : the density of water
V: the volume of the particle
D: the diameter of the particle
g: acceleration due to gravity

The weight of the particle (1a) and the buoyancy of the particle (1b) have similar expressions, both relevant to volume and density. Weight and buoyancy are essentially forces due to gravitational pull acting on the particle and the water, which always have opposite directions. Therefore, the two forces can be combined into a single force, the effective weight of the particle (2).

$$EffectiveWeight = F_G - F_B = (\rho_s - \rho_w)Vg = \frac{1}{6}\pi(\rho_s - \rho_w)D^3 g \tag{2}$$

The effective weight summarizes the hydrostatic forces that keep the particle sedimentary when no water flow is present. Notice that the particle density in comparison to the water density determines the direction of effective weight. Those particles with a lower density than water are not the subjects of the resuspension study for they always float due to negative effective weights.

Remember the root cause of sediment resuspension are the hydrodynamic forces brought by flowing water currents. When water flow by a particle on the sediment, it hit the particle and divert. The diversion produces uneven water velocity distribution around the particle. Water under the particle and near the upstream face of the particle have lower velocities compared to water on top and behind the particle. According to Bernoulli's law, a lower velocity results in a higher pressure area. The pressure difference can be represented by two hydrodynamic forces: lift force (3a) and drag force (3b).

Lift force is perpendicular to the direction of the flow while drag force is opposite to the direction of relative velocity between the particle and water.

$$F_L = C_L \frac{1}{2} \rho_w A U^2 = C_L \frac{\pi}{8} \rho_w D^2 U^2 \tag{3a}$$

$$F_D = C_D \frac{1}{2} \rho_w A U^2 = C_D \frac{\pi}{8} \rho_w D^2 U^2 \tag{3b}$$

where:
A : the area of the largest cross section of the particle perpendicular to the direction of the water flow
U : the speed of the particle relevant to water
C_L: lift coefficient
C_D: drag coefficient

(3a) and (3b) are derived from the conservation of energy. C_L and C_D are the coefficients of lift and drag, respectively. The coefficients can be determined by carrying out experiments. The coefficients are relevant to the particle geometry, the flow condition, and many other factors.

Whether or not a particle will resuspend can be induced from the forces acting upon it. However, it is impossible to determine the precise magnitude and direction of every force at every moment of the resuspension process. A reasonable simplification is therefore established to describe the tendency of resuspension of a sediment particle.

$$ResuspensionTendency = \frac{PromotingForces}{ResistingForces} \approx \frac{LiftandDrag}{EffectiveWeight} = K \frac{\rho_w}{\rho_s - \rho_w} \frac{1}{gD} U^2 \tag{4}$$

where K is a coefficient representing the combined effect of lift and drag coefficent.

The resulting ResuspensionTendency is a ratio between the promoting forces and the resisting forces in the resuspension process. From the expression (4), we can isolate the elements influencing the resuspension: density difference, particle diameter, lift and drag conditions, and the flow velocity. It is obvious that a lower effective density, a smaller particle diameter, or a higher water speed can all increase ResuspensionTendency. However, it is not easy to determine the value of K through pure analysis, more often, we find this value through experiments. Also, this expression of ResuspensionTendency is unable to incorporate the influences of other factors such as cohesive forces and friction. Though they are formerly ignored for not being the dominant factors, they still exist and can have some influence.

2.2 An Experiment Based Model: Shields Diagram

Due to these uncertainties, empirical models based on experiments are often preferred over pure theoretical models for engineering purpose. One authoritative, commonly referenced model is the Shields diagram proposed by Albert Frank Shields. Shields defined a Shields Parameter representing to determined the initiation of motion of sediments.

$$\tau_c^* = \frac{\tau_{bc}}{\rho_w g R D} \tag{5}$$

where:
τ_c^* : Shields Parameter
τ_{bc} : Critical bed shear stress
$R = \frac{(\rho_s - \rho_w)}{\rho_w}$: effective density ratio of the particle when submerged in water

The Shields Parameter is a non-dimensional number. By changing its form, we can get a more thorough understanding of it.

$$\tau_c^* = \frac{\tau_{bc}}{\rho_w g R D} \tag{6a}$$

$$= \frac{\tau_{bc} D^2}{(\rho_s - \rho_w) g D^3} \tag{6b}$$

$$= \frac{Criticalbedshearforce}{Particleeffectiveweight} \tag{6c}$$

Expression (6c) is surprisingly similar to the previous definition of ResuspensionTendency, indicating that ResuspensionTendency and Shields Parameter are essentially describing the same physical property, which is the ease of resuspension. However, there is difference between the two numbers: ResuspensionTendency is derived from force analysis, while the value of Shields Parameter is based on experiments. For ResuspensionTendency, the higher the value, the easier the occurrence of resuspension. Contrarily, for Shields Parameter, the lower the value, the easier the occurrence of resuspension. This is because the numerator of Shields Parameter is *critical* bed shear stress, meaning the stress needed for the sediment to resuspend. Low Shields Parameter therefore means resuspension can be reached at a low critical shear stress over effective weight ratio.

The connection between ResuspensionTendency and Shields Parameter can be even clearer when we include the following equation:

$$\tau_{bc} = \rho_w u_{*c}^2 \tag{7}$$

where u_{*c} is the critical shear velocity.

$$\tau_c^* = \frac{\tau_{bc}}{\rho_w g R D} \tag{8a}$$

$$= \frac{\rho_w u_{*c}^2}{(\rho_s - \rho_w) g D} \tag{8b}$$

Through experimenting with particles of different densities and sizes, Shields discovered Shields Parameter to be a function of the particle Reynolds number Re_p and drew a graph, Figure 2.2, known as Shields Diagram.

$$Re_p = \frac{u_{*c} D}{\nu} \tag{9}$$

where ν is the kinetic viscosity of water.

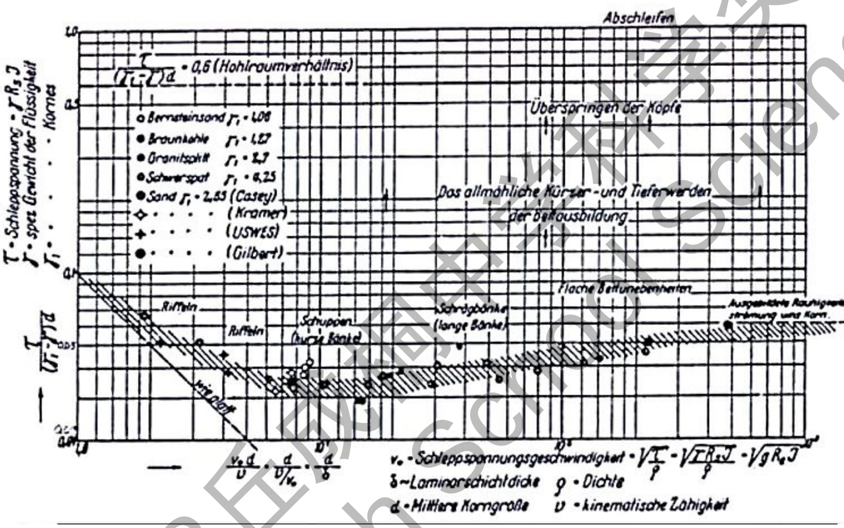

Figure 2.2: The Original Shields Diagram. Show the relationship between the Shields parameter τ_c^2 and particle Renolds number Re_p. The curve is approximately linear at left, saddle-shaped at middle, and approaches a constant value at right.

However, the particle Reynolds number isn't convenient enough for determining the Shields number due to its dependency on the critical shear velocity. Some researchers later constructed a replacement, D_*, for the particle Reynolds number to eliminate the dependency, switching measuring critical shear velocity to measuring more direct physical properties, the particle density and diameter. A reformed Shields diagram is shown in Figure 2.3.

$$D_* = \left[\frac{g(\rho_s - \rho_w)}{\nu^2}\right]^{\frac{1}{3}} D \tag{10}$$

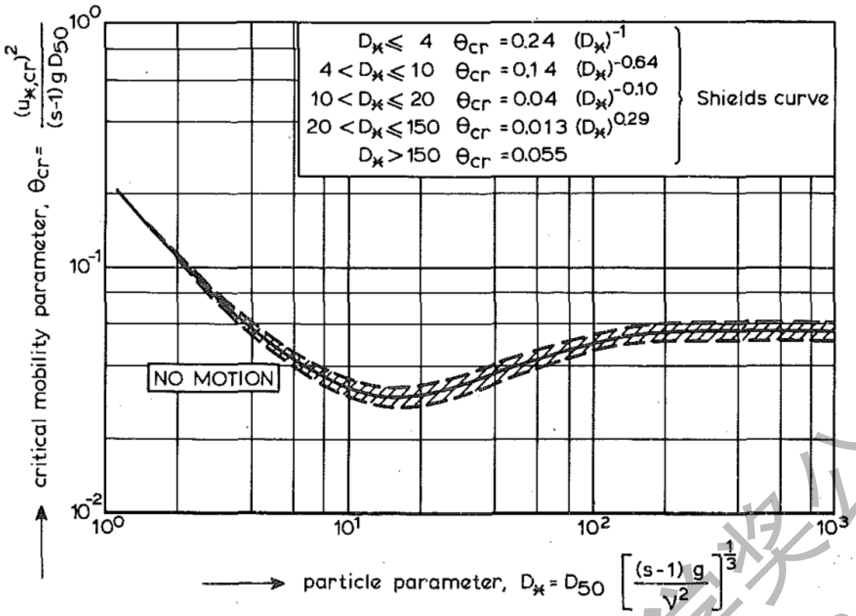

Figure 2.3: A reformed shields diagram according to Van Rijn.[10] The x axis is switched to D_* instead of Re_p.

2.3 Applying the Model: Find Patterns and Make Predictions

Now, using the reformed Shields Diagram, by inputting the value of particle diameter and particle density, we can get a predicted value of the critical shear velocity, or critical shear stress. A Matlab code is used to automate this process, shown in Figure 2.4.

```
%Resuspension Shear Velocity Calculator
V = Get_Shear_Velocity(100,2500) % Call the function, recieve the result as V

function critical_shear_velocity = Get_Shear_Velocity(D, rho) % Function definition, two input parameters
    % Calculate D*
    % Input D is in micrometer, convert to meter
    D_star = (9.81*((rho-1000)/1000)*10^12)^(1/3)*(D*10^-6);
    % Find Shields Paramter using a piecewise fit according to Van Rijn
    if(D_star <= 4)
        shields = 0.24*(D_star)^-1;
    elseif(D_star <= 10)
        shields = 0.14*(D_star)^-0.64;
    elseif(D_star <= 20)
        shields = 0.04*(D_star)^-0.1;
    elseif(D_star <= 150)
        shields = 0.013*(D_star)^0.29;
    else
        shields = 0.055;
    end
    % Get critical shear velocity
    critical_shear_velocity = sqrt(shields*((rho-1000)/1000)*9.81*(D*10^-6));
end
```

```
命令行窗口
  V =

    0.0120
```

Figure 2.4: A function called Get_Shear_Velocity is defined. By calculating D_* and Shields Parameter step by step according to previous formula, we can get the theoretical shear velocity needed for resuspension. For example, for particles that has 100 μm diameter and 2500 kg/m^3 density, it is predicted to resuspend at a shear velocity of 0.0120 m/s.

By repeating that calculation for a range of different particle diameters and densities, we can draw a surface,

Figure 2.5, that visualizes the critical shear velocity's relation with diameter and density.

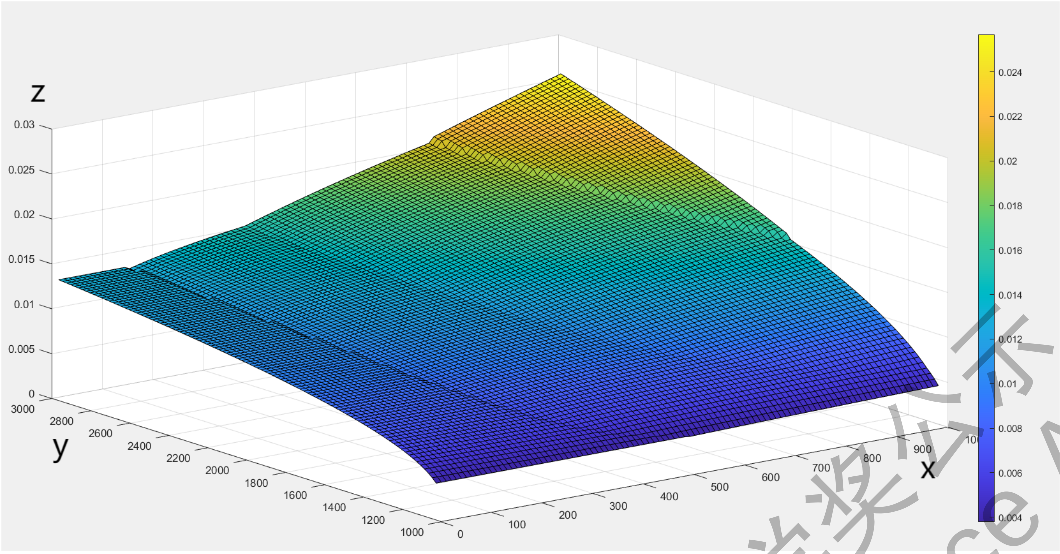

Figure 2.5: Visualize critical shear velocity: Every point on this surface, located by a three dimensional coordinate [X,Y,Z], represents one calculation. X stands for its diameter, Y stands for its density, and Z is its resuspension critical shear velocity. The height of the points suggests its ease of resuspension. The higher the point, the larger the critical shear velocity, the harder the resuspension.

The curving shape of this surface can lead us to some conclusions: 1) According to Figure 2.5, the larger the density, the larger the diameter, the harder resuspension is. 2) According to Figure 2.6(a), At low densities, density become the dominant factor controlling resuspension. It is easy to notice a steep slope that bends the surface downward at low densities. For example, when density is at 1050 kg/m^3, the critical shear velocity never exceeds $0.005 m/s$ even if diameter reaches $1000 \mu m$. 3) According to figure 2.6(b), At small diameters, especially when diameter is lower than $200 \mu m$, the increase in diameter has minor effect on the critical shear velocity. For example, at density $2500 kg/m^3$, the critical shear velocity of diameter $100 \mu m$ is $0.0120 m/s$. Even though the diameter doubles to $200 \mu m$, the critical shear velocity only increase to 0.0122, an increase less than 2%.

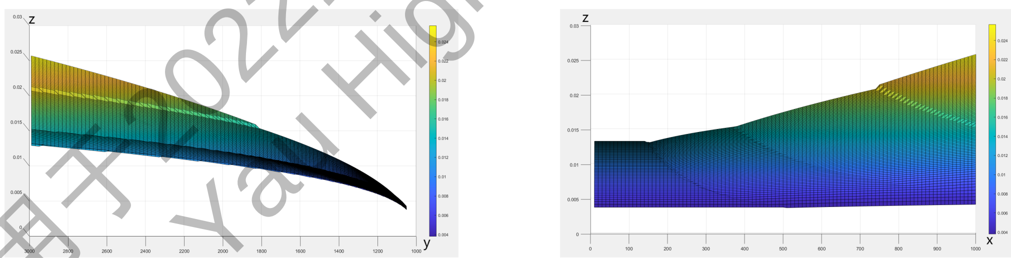

(a) (b)

Figure 2.6: figure (a) leads to conclusion (2): view the 3D graph from the Y-Z plane, we see the influence of density. At low densities, the surface is bent downward. figure (b) leads to conclusion (3): view the 3D graph from the X-Z plane, we see the influence of diameter. At low diameters, the slope is mild.

Finally, with all the conclusion drawn from force analysis and the Shields diagram, we can predict how will microplastic-sediment aggregates change the resuspension. Microplastics are of low densities, so the overall density of the aggregates must decrease, lowering resuspension critical shear velocity. But forming aggregates also means increased particle sizes, which increases resuspension critical shear velocity. But the probability of density change being the dominant factor is large, so the hypothesis is that microplastics will make resuspension easier.

3 Experiment

The experiment part is designed to the test our theory. First, microplastic-sediment aggregates are prepared. Then, some preparatory measurements are done to get information about the size and density, two important factors affecting resuspension, of the raw sediment, microplastic, and the aggregates they form. Finally, we conduct the main experiment, which is testing the resuspension critical shear velocity by exposing the sediments under various water velocities. We want to see how the critical shear velocity will change after microplastics are added to the sediments and form aggregates.

3.1 Prepare Microplastic-Sediment Aggregates

Five groups of experiments are designed to test the effect of microplastic-sediment aggregates' influence on resuspension critical condition. The independent variable being altered across the five groups is the concentration of microplastics added. The dependent variable is the resuspension condition. The five groups each has microplastic concentration of 0, 5000, 10000, 20000, and 30000. Concentration is measured in the number of particles added. 0 concentration means no microplastic is added, thus a control group for reference. 200 grams of dry river sand is added to each of the five identical 1000 mL beakers. Then, 500 grams of water is added to each beaker. After that, different concentrations of microplastics are added according to the labels of the beakers.

River sand used in the experiment was extracted from a local river bed directly. The location of the river is shown in Figure 3.1.

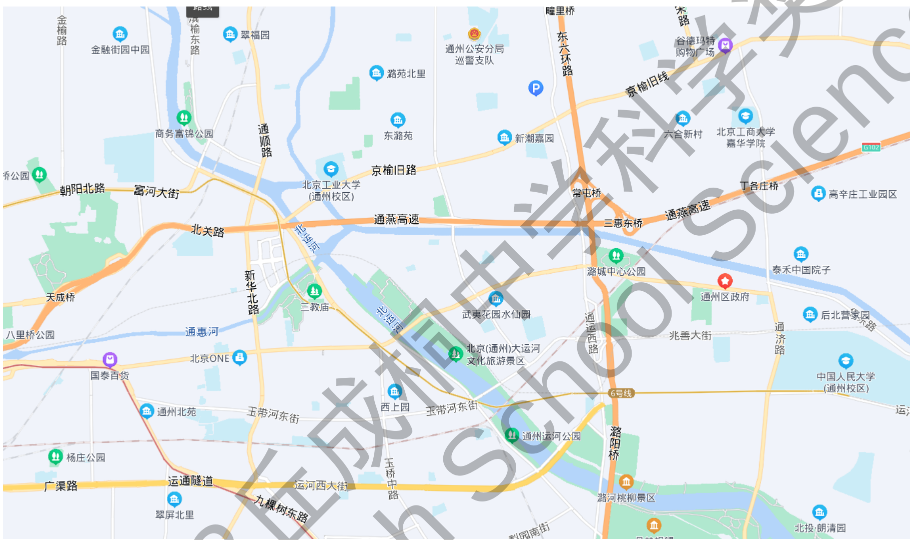

Figure 3.1: Map: The Grand Canal,Tongzhou, Beijing

Shown in Figure 3.2, sediments near the river bed surface were dug using bowls. Only the sediments on the top 5cm were selected, for they are in contact with the water readily and make up the majority of the resuspended materials, which is our object of study. A minor deviation might be caused due to the location of the sediments extracted: we were only able to obtain near shore sediments due to operation difficulty. It was impractical to acquire sediments in the middle of the river. However, river sediment near-shore or in-the-middle do not differ greatly in their size and other properties, for the river we investigate has not wide enough channel width.

Figure 3.2: Dug the river sand.

It is worth mentioning the method of counting microplastics. Microplastics, suggested by their name, are tiny. Counting out thousands of them directly is impossible work load. Thus, its number has to be transformed into other more manageable quantities. Mass is first considered, however, the precision of ordinary balance is too limited. The difference in mass between 5000 and 10000 microplastics is not discernible.

Figure 3.3: Count plastic with a straw. The left photo shows the initial 500 microplastics counted out. Using its height, 2mm, as a benchmark, 10000 microplastics is 4cm.

Volume proves to be a better method. A thin, transparent straw is used. 500 microplastics is first counted out, added into the straw, which forms a cylinder of 2mm high, shown in Figure 3.3. Through this way, a correlation is built: 500 is 2mm, number into volume into height, and height is easy to measure. 5 mL of concentrated microalgae is added to each beaker. Microalgae are used to facilitated the aggregation process. Finally, the ingredients in each beaker are fully stirred with a rod. The process is shown in Figure 3.4.

Figure 3.4: Adding sand to the beakers. Add Water and microalgae. Stir. White foaming layer floating on top of water is consist of bubbles and microplastics. The higher the concentration of microplastics, the larger area the foam covers.

The beakers are sealed with plastic films to minimize water loss due to evaporation. Holes are left open on the films to allow air exchange. The beakers are lined up on the balcony and left still. Every three days, the beakers are fully stirred to increase the chance of contact between the microplastics and the sediments. Microplastics are afloat on the surface of the water at first. As time passes, aggregates start to form, and the microplastics sink down into the sediments. The process of aggregation continued for about a month for the microplastics on the surface to reduce to nearly zero. The first two stages of aggregation is shown by Figure 3.5 and 3.6.

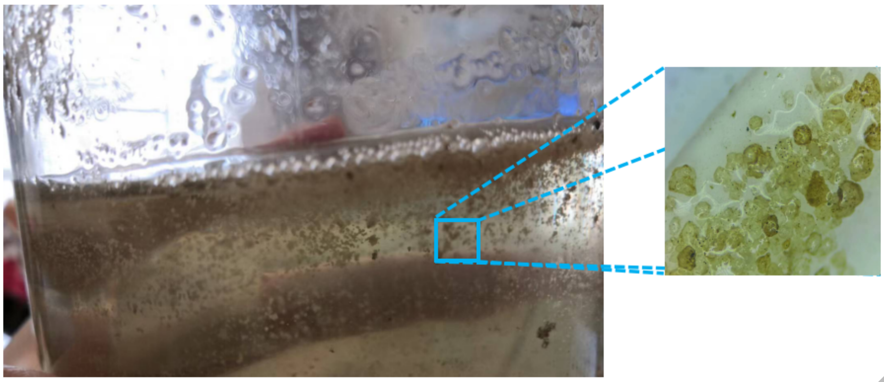

Figure 3.5: Stage 1: Microplastics become wrapped in a coat of microalgae, giving them a light green color. This process takes about one week.

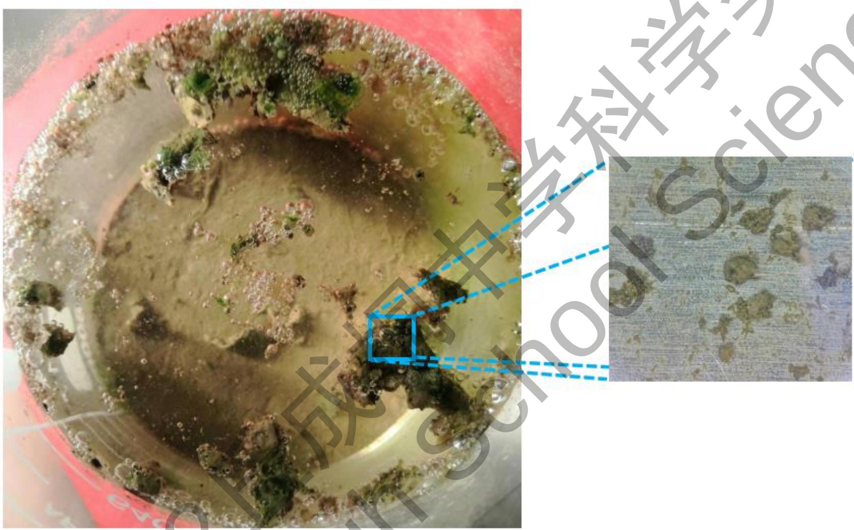

Figure 3.6: Stage 2: Microplastics coated with algae traps sediment particles(sand and mud), forming larger aggregates. When the aggregates acquire enough weight, they sink down and become part of the sediment. This process takes about three weeks.

Though microalgae is an effective accelerator for microplastic-sediment aggregation, it needs to be removed after the formation of aggregates. There are two reasons for this: 1) Microalgae not only bind with microplastics, but also the beaker walls. It blocks our view, which will severely interfere with the observation of turbidity in the following experiment. 2) When microalgae thrives, it can form large "blankets" with the sediments. Those blankets can significantly change the resuspension process and blur the influence of microplastic-sediment aggregates. To remove the microalgae, after the aggregation, the beakers are fully stirred again and moved into a box to prevent the microalgae from sunlight,shown in Figure 3.7. The regular stirring is canceled during the dark process stage. A week later, most microalgae are removed. The preparation of aggregates finished at this stage. The 5 groups of beakers are ready for resuspension experiment.

Figure 3.7: Stage 3: The beakers are under dark process for a week. The microplastics-sediment aggregates are now settled inside the sediments.

3.2 Preparatory Measurements

3.2.1 The Size of the Particles

The size of the particles is a critical factor for resuspension. The diameters of pure river sand, pure microplastics, and aggregations of sediment and microplastics are measured.

First, the particles are sampled. Dry Sand and microplastics are sampled directly. Particles of the sediment surfaces of the five groups of experiments are scoured with a spoon, then spread on to a board and let dry, as shown in Figure 3.8. After sampling, the samples are observed under a 40x microscope and photos are taken, shown in Figure 3.9. Finally, the photos are analyzed by software Imagej to get the average sizes of the particles.

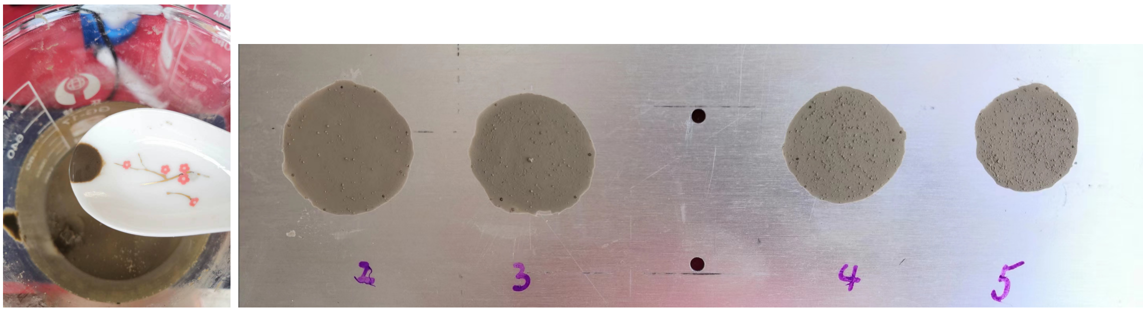

Figure 3.8: The sediment surface samples.

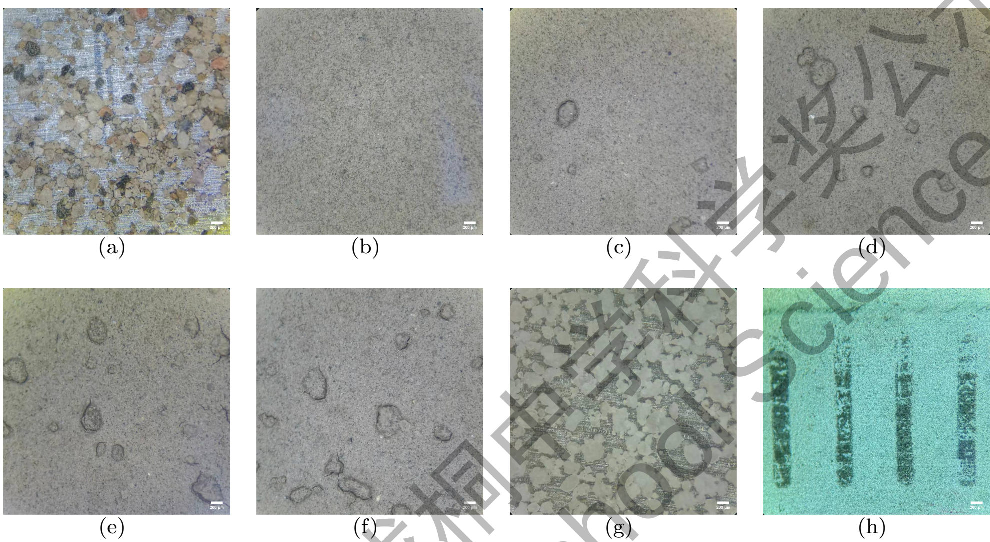

Figure 3.9: Particles observed under a 40 × microscope. (a) sand particles (b) fine sand particles at the surface of the sediment bed(no microplastic added) (c) 5000 microplastics added (d) 10000 (e) 20000 (f) 30000 (g) raw microplastic particles (h) a ruler, used for building a length scale

	Aggregates	**Microplastics**	**Sand**
25%	135.5	122.9	78.5
50%	173.6	163.0	117.5
75%	267.0	219.1	144.8
mean	218.3	172.2	118.2
std	111.2	66.2	46.5

Table 1: The Statiscal Characteristics of the Sizes of Different Particles. x% means the x percent of data. std is the standard deviation. All data in unit micrometer.

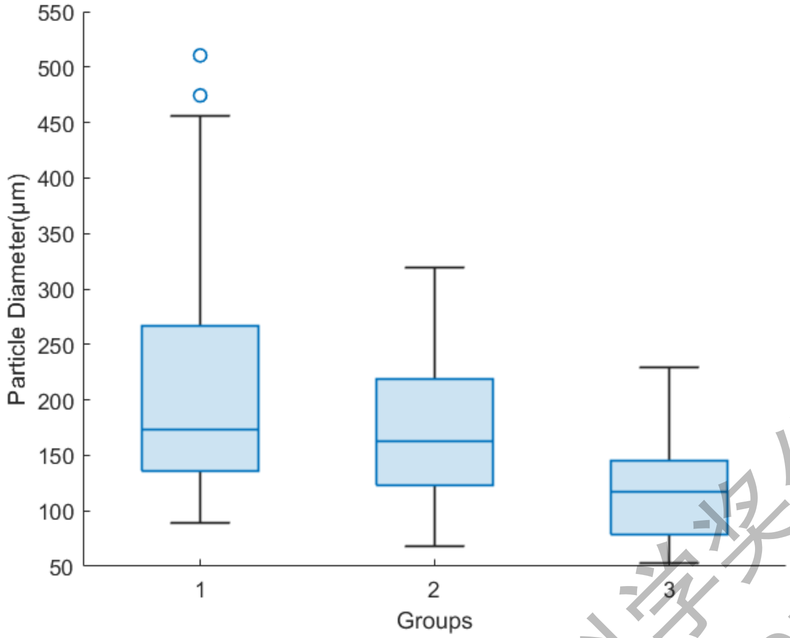

Figure 3.10: A box chart showing the distribution of the size data. Group 1 stands for Aggregates, Group 2 Microplastics, Group 3 sand.

From Table 1 and Figure 3.10, we can draw the following conclusions: 1) The general size of the particles follows the order of Aggregates larger than Microplastics larger than Sand. 2) The size distribution of aggregates is much more spread compares to that of microplastics and sand. Combining 1) and 2), as well as the photos taken, we can reasonably infer that microplastic-sediment aggregates are usually formed by a single microplastic enclosed by many fine sand particles. The size of the aggregates cover a wider range because the size of the enclosed microplastic, and the thickness of the fine sand shell, can both vary.

3.2.2 The Density of the Particles

The other determining factor aside from particle size is the particle density. For a particle as small as a grain of sand, measuring density can be even more difficult than measuring length. According to the definition of density, mass over volume, measuring the density of one single particle directly is impossible due to the limited precision of the instruments. Therefore, some indirect measures are applied to work out the density of the particles.

For microplastics, because they are bought online with the type of plastic, PE, specifically stated, no measurement is required. The particle density is equal to the material density of PE, which is about 900 kg/m^3.

The density of pure river sand is measured by following these procedures, shown in Figure 3.11: First, M1 of sand is sampled out using an electric balance and poured into a flask; Then, water was added to the flask while stirring thoroughly to reach a certain volume V1, and the total mass M2 is recorded; After that, the flask is cleared; Finally, only water is added to the flask to reach volume V1 again, and the mass M3 is recorded. This method is designed to expel the air inside the porous dry sand to get the real density of the sand instead of its bulk density. The real density of sand can be calculated using the following formula:

$$\rho_{sand} = \frac{M1}{(M2 - M3)/\rho_w} ZZ \tag{11}$$

Figure 3.11: The procedures of measuring sand density.

In this measurement, M1 = 50g, M2 = 220g, M3 = 190g, yielding a density of $2500 kg/m^3$.

As for the density of microplastic-sediment aggregates, another method is applied. By measuring the terminal velocity of the aggregates in water, particle density can be related to particle size and terminal velocity, both values we can measure. The method of calculating the density of the aggregates based on the density of sand and microplastics is not realistic because we don't know the ratio of sand and microplastics in a aggregate. This ratio can be different across the aggregates as well, a conclusion mentioned in the last section. The method of measuring sand density is neither applicable for the case of aggregates. Aggregates only exist in a thin top layer of the sediment. The total mass of all aggregates may not exceed a few grams. Considering the precision of the instruments, this method is abandoned.

The terminal velocity method is based on force balance of a particle settling in water. A particle is release into still water at zero velocity. Three forces guides the movement of the particle: weight of the particle, buoyancy of the particle, and hydrodynamic drag exerted by water. Weight and Buoyancy remain constant during the falling process, while Drag increases as the relative velocity of the object to water increases. Thus, the three forces reach balance when the magnitude of drag and buoyancy equals to the magnitude of weight. The velocity of the object remains constant as well at the balance state, which is termed the terminal velocity. Quantified expression are as follows:

According to the Stoke's Law, the force of viscosity on a small sphere moving through a viscous fluid is given by:

$$F_d = 3\pi\mu DU \tag{12}$$

Where μ is the dynamic viscosity of water.

Recall previous expression of weight and buoyancy and effective weight, the balance state can be described as:

$$F_d = EffectiveWeight \tag{13a}$$

$$3\pi\mu DU = \frac{1}{6}\pi(\rho_s - \rho_w)D^3 g \tag{13b}$$

$$U = \frac{1}{18}\frac{\rho_s - \rho_w}{\mu}D^2 g \tag{13c}$$

The equation (12c) successfully connects particle density to settling velocity and particle diameter, quantities we both know.

To measure the settling velocity of aggregates, the following steps are taken, shown in Figure 3.12: 1) a long, transparent tube is prepared. On one side the tube is blocked by rubber, the other side left open. The tube is marked with lines set 1cm apart. 2) The tube is hold stationary, vertical to the ground, making sure the water column has zero velocity. A camera parallel to the center of the tube is used for taking video. 3) A small spoon of sediment is slowly released into the water column by submerging the spoon under the water surface. Then, the particles are allowed to settle, whose motion is recorded by the camera. 4) After recording, the video is analyzed using the program Tracker, which is a physic tool for tracking moving objects. 30 particles' path are analyzed as samples. Their terminal velocity are calculated and averaged to get a representative terminal velocity of all aggregates.

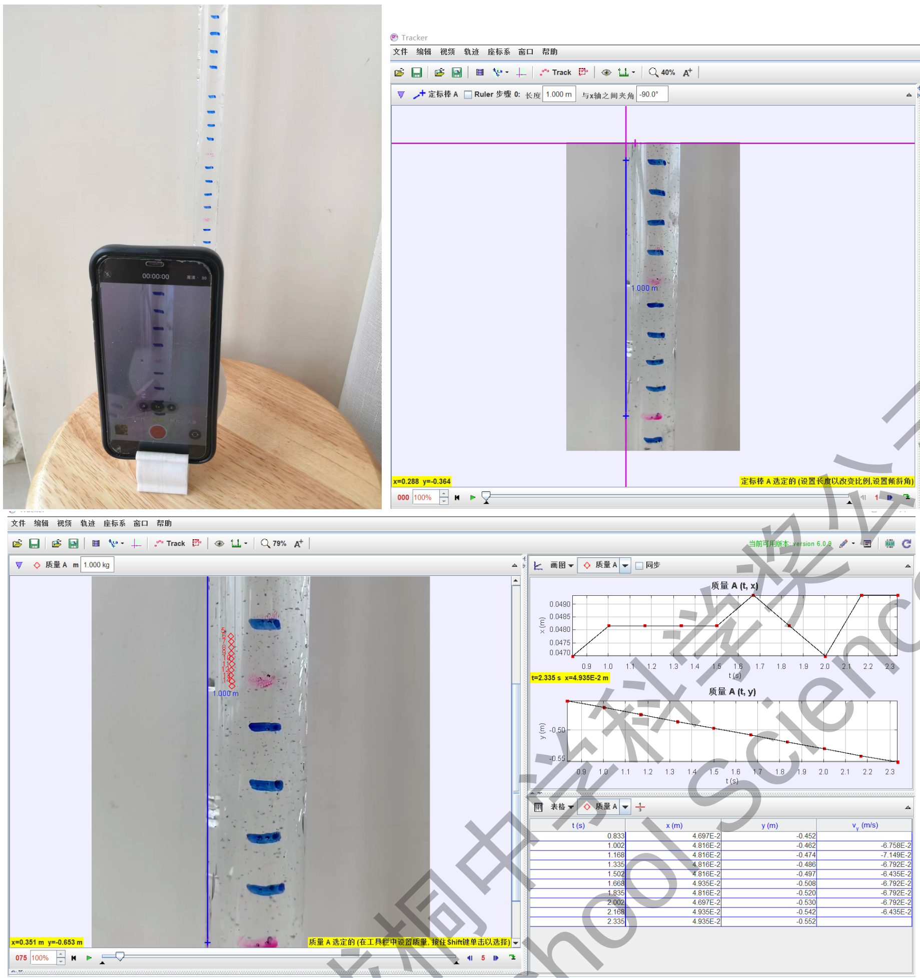

Figure 3.12: Filming the settling process of the aggregates and analyze their velocity with Tracker.

Mean Velocity(cm/s)	Std
4.622	1.297

Table 2: The average settling velocity and the standard deviation of the aggregates.

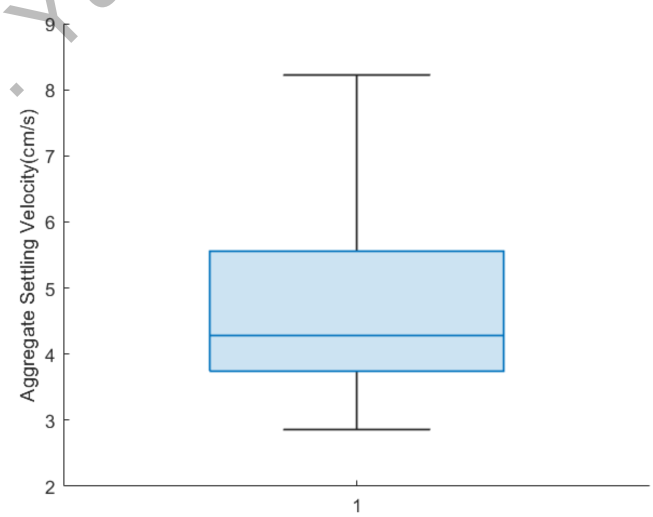

Figure 3.13: A box chart of the settling velocities of the aggregates.

Now, use equation 12(c), fill in U and D with acquired data in Table 2, we get the density of the aggregates:

$$0.004622 = \frac{1}{18}\frac{\rho_s - \rho w}{\mu}(218.3 \times 10^{-6})^2 \times 9.81$$

$$\rho_{aggregates} \approx 1200kg/m^3$$

3.2.3 Prediction Based on Information

Now, with all information at hand, we can predict how resuspension critical shear velocity might change based on the theory we proposed. The size and density of sand and microplastic-sediment aggregates are summarized in the Table 3:

	Sand	Aggregates
Diameter(μm)	118.2	218.3
Density(kg/m^3)	2500	1200

Table 3: The mean diameter and density of sand and microplastic-sediment aggregates.

By plugging the numbers into the Shields Calculator we designed in the theory section, we get two critical shear velocities, shown in Table 4:

	Sand	Aggregates
Predicted Critical Shear Velocity(m/s)	0.0120	0.0061

Table 4: Predicted Critical Shear Velocities

Will our experiment confirm the two predictions?

3.3 Build the Resuspension System: Where We Hold the Main Experiment

The resuspension system is consist of three parts: The speed controller, lighting and support, and the data recording camera. The speed controller is mainly a DC motor that spins the water, shown in Figure 3.14, plus a programmable Arduino development board that changes the speed of the motor, shown in Figure 3.15.

Maximum Speed(rpm)	**Rated Current(A)**	**Rated Voltage(V)**
200	2.5	12

Table 5: Motor Parameters

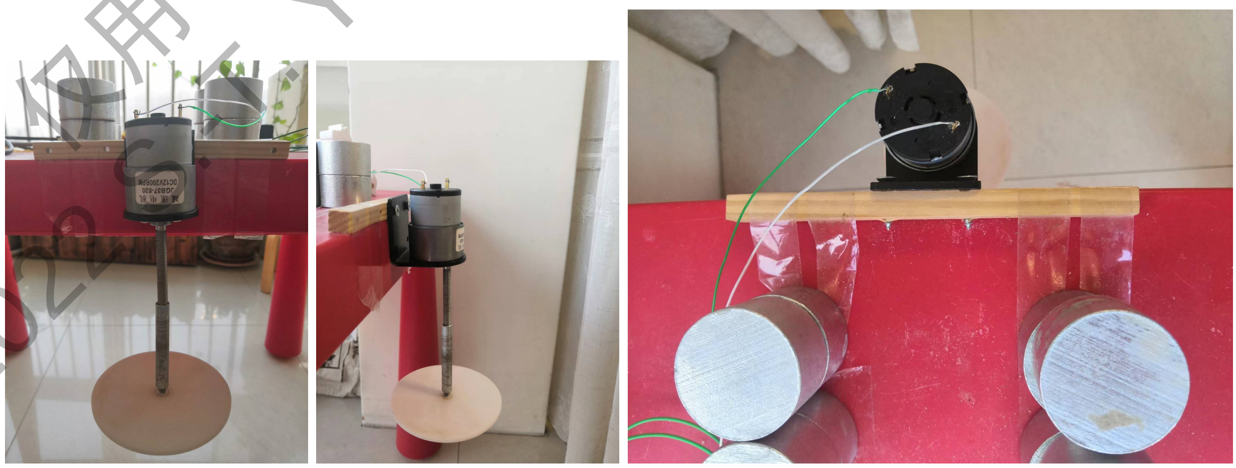

Figure 3.14: The Photos of the motor and the disk spinner, fixed on to a table (**a**) The front view of the spinner,the disk is linked with the motor by iron axis (**b**)The side view of the motor,the motor is nailed onto a piece of wood(**c**)The top view of the motor, tapes and weights are used for stabling

To simulate the resuspension process and find out the critical shear velocity of resuspension, the water is being spinned at increasing velocities. A velocity control command based on time is created. Formally, a voltage transformer and a knob were controlled manually. This method required the experimenter to supervise the process and rotate the knob every two minutes, which was imprecise and laborious. Later, the system is automated by constructing a programmable Arduino singlechip.

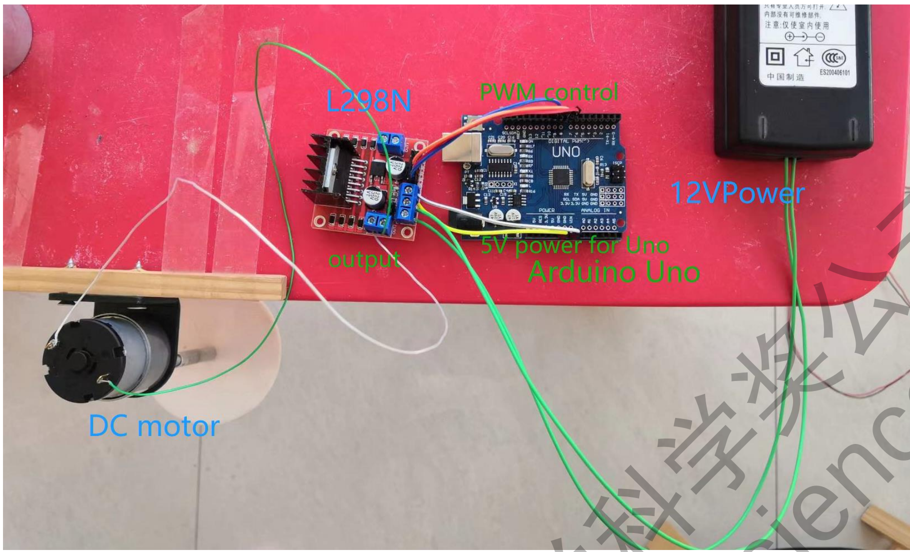

Figure 3.15: The Arduino singlechip control: motor is linked to a L298N chip, which is controlled by Uno through PWM(Pulse Width Modulation)

The Arduino Uno is programmed through its corresponding software. Basically, the speed of the motor is increased every two minutes by a writing a for loop.

The lighting and support system aid the observation, shown in Figure 3.15. A lamp is placed directly on top of the beaker. Light of constant intensity is emitted from the lamp, penetrating the water from top. White paper is used as a background. A piece of paper is hanged below the table, behind the beaker; another piece is under the beaker. A chair is used for placing the beaker, ensuring the disk spinner is immersed in the water at an appropriate height. Light mostly enters the water from the top, then being scattered toward sides. There also may be some light bouncing back from the paper, then enters the beaker and being scattered. Regardless how many paths can light penetrate the beaker and be received by the observe window, the amount of light reaching the observe window is always the same when no resuspension occurs.

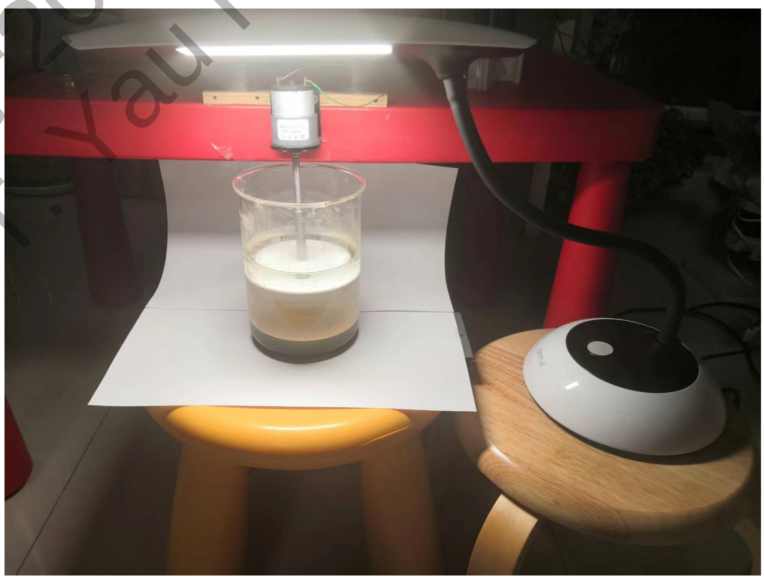

Figure 3.16: Lighting and support system.

The data recording system is a DSLR placed on a chair which takes photos of the beaker, shown in Figure 3.17. The photos will be used as indicators of the scale of resuspension by analyzing the darkness of the photos.

Therefore, fixed camera parameters are used under the M mode to strip the influence of different exposures.

ISO	shutter speed(s)	f-number	focal length(mm)
500	1/80	5.6	105

Table 6: Camera Parameters

The shooting is also automated. Using the interval shooting function of the camera, photos are taken at the end of every two minutes of the spinning.

Figure 3.17: The camera placement and the interval shooting settings.

A general view of the whole system is shown in Figure 3.18.

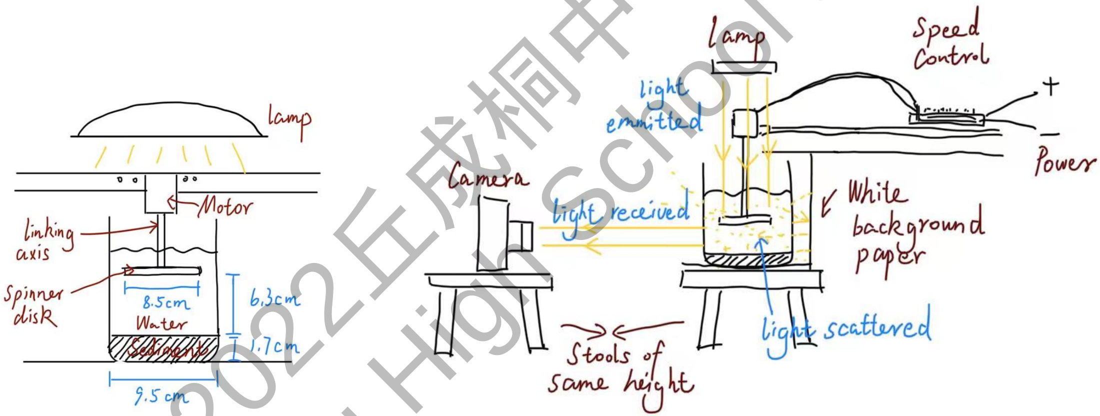

Figure 3.18: The frontal view and the side view of the whole resuspension system.

3.4 Carry Out the Experiment

After constructing the resuspension system, the experiment is carried out. The procedures are shown in a flow chart, shown in Figure 3.19. First we fully stir the sediments in the 5 beakers(control group, experiment groups with microplastic concentration of 5000, 10000, 20000, 30000). We allow two days of settling, which is enough time for the water to turn clear. After settling, We put a beaker at the right position, with the spinner submerged in the water. Then we start the automatic spinning and photo shooting. The spinner will go through a series of seventeen velocities(0,36,48,60,72,84,96,102,108,114,120,126,132,138,144,150,156 rpm), maintaining each velocity for two minutes. At the end of every two minutes, the camera will shoot to record the turbidity. The process is repeated for the rest 4 beakers. Finally, we clean up and put the beakers back to the dark box. The photos are saved for analysis. The full experiment is repeated three times.

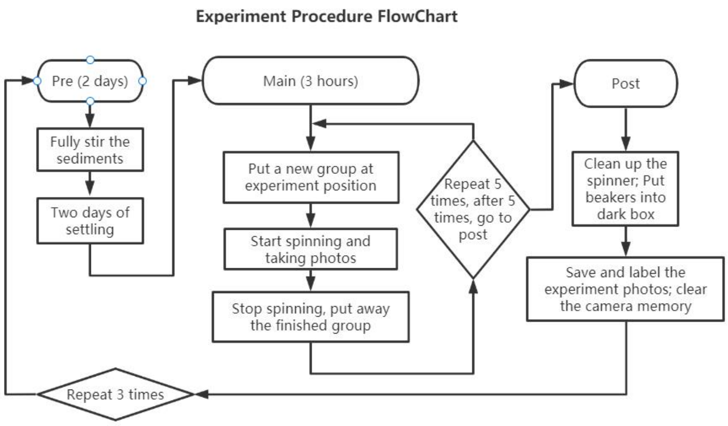

Figure 3.19: The procedures of the resuspension experiment summarized as a informal flowchart.

3.5 Experiment Data: Results and Analysis

3.6 Raw Data

The raw data we get from the experiments are sets of photos, each representing the resuspension condition of one group of sediments at a certain velocity. The photos can be arranged into three tables(repeated 3 times), each table having 5 rows(5 groups) and 17 columns(17 velocities). Figure 3.20 shows the photos of the first table. The other two tables are in the appendix.

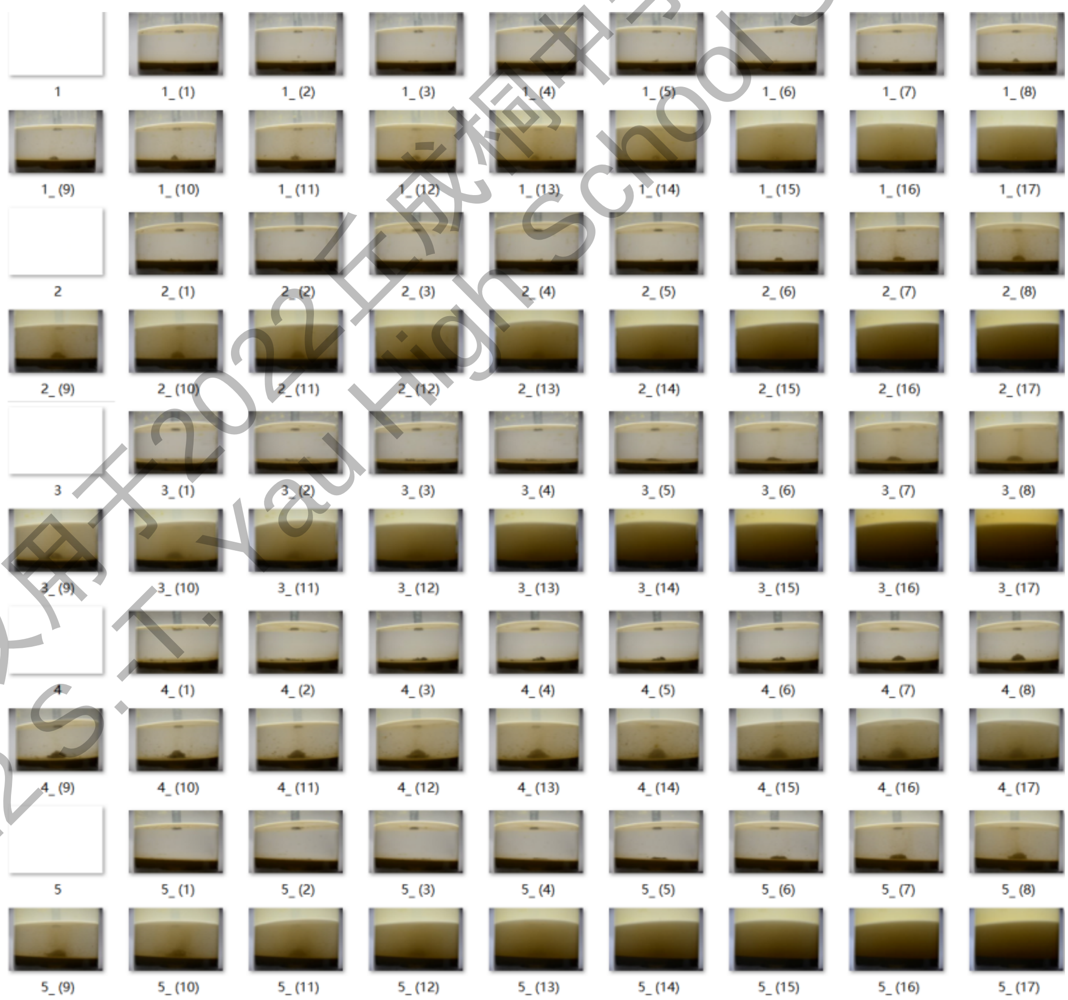

Figure 3.20: Raw photos acquired from the first experiment. The white images mark the beginning of each group. The 17 columns divided into 2*9 columns to see clearer.

3.6.1 Find Bed Shear Velocity

When describing the condition of particle resuspension, we mentioned *critical shear velocity* as the velocity of water that initiates the motion of the particle. However, water doesn't flow above the river bed at a uniform velocity. The velocity of the water at the river surface differ from the velocity of the water 1 meter deep, and the velocity of the water near the river bed. To preserve the uniformity of sediment resuspension studies, we agree that critical shear velocity refers to the velocity of water at the river bed. However, it is impractical to measure the speed of water at the river bed. Thus, a velocity profile that describes the velocity of water at different depth of a river needs to be established. For our experiment, a relationship between the spinner velocity and the bed shear velocity is needed. Luckily, there's a existing law describing this kind of problem, the Law of the Wall. First published by Theodore von Kármán, the Law of the Wall states that the velocity of flow has a logarithmic relation with the distance from the fluid boundary, *the wall*. The flow velocity ditribution can be desribed by the following equation:

$$\frac{u}{u_*} = \frac{1}{\kappa} \ln \frac{h}{h_0} \tag{14}$$

where
u = flow velocity
u_* = bed shear velocity
κ = von Kármán's constant, approximately 0.41
h = the distance from the boundary
h_0 = bed roughness height where the flow velocity goes to zero

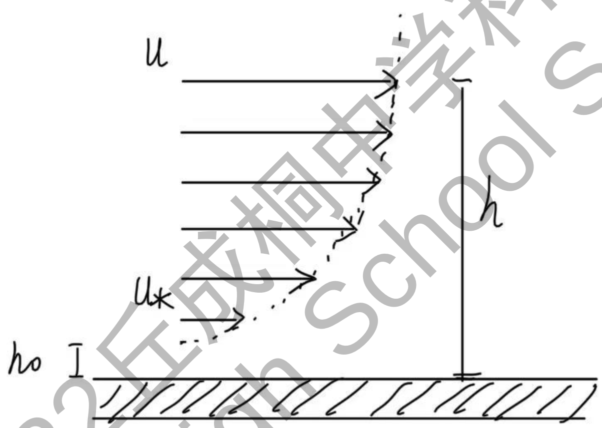

Figure 3.21: The Law of Wall

Figure 3.21 illustrates the flow velocity distribution near the wall predicted by the Law of Wall.

The size of the sediment is small enough in our experiment, so the condition is categorized as hydraulically smooth flow and follows this description:

$$h_0 = \frac{\nu}{9u_*} \tag{15}$$

Now we can start converting spinner velocity into bed shear velocity: First, the angular velocities of the spinner is transformed into the water's linear velocity. Due to the cylindrical shape of the beaker, the water with a greater distance from the disk center spins faster. So we pick the velocity at midway of the spinner disk as an average water flow velocity. Assuming no-slip condition, by multiplying the angular velocity with half of the disk diameter, 4.25 cm, we get the flow velocity u. After that, solve for $u*$ with u and other know constants. Table 7 shows the velocity sequence tested in the experiment in the form of spinner velocity and shear bed velocity.

spinner velocity(rpm)	water flow velocity(m/s)	bed shear velocity(m/s)
0	0	0
36	0.08007	0.004220
48	0.1068	0.005449
60	0.1335	0.006647
72	0.1601	0.007817
84	0.1868	0.008974
96	0.2135	0.01011
102	0.2269	0.001068
108	0.2402	0.01124
114	0.2536	0.01180
120	0.2669	0.01236
126	0.2802	0.01291
132	0.2936	0.01346
138	0.3069	0.01401
144	0.3203	0.01456
150	0.3336	0.01510
156	0.3470	0.01565

Table 7: The tested velocity sequence converted from spinner velocity into water flow velocity and bed shear velocity.

By imposing these bed shear velocities to the sediments, we observe the resuspension condition and determines which shear velocity should be the critical shear velocity that initiates the motion. So, how can we describe the resuspension condition? This is done by analyzing the turbidity of the water.

3.6.2 Analyze Turbidity

The data we have are series of photos, which are composed of matrices of pixels. The data we want are numbers describing the turbidity of water, or the concentration of resuspended particles in the water column. The two sets of data can be connected through an optical method, the Beer-Lambert Law. Beer-Lambert Law states that the concentration of a solution is linearly proportional to the absorbance of light transmitting through the solution. As light penetrate a solution, or a mixture that has particles suspending, the light is scattered. The light intensity before and after the penetration changes. The degree of light intensity drop is affected by three factors: the solution concentration, the penetration length, and the absorptivity of the material.

$$A = -\lg \frac{I}{I_0} = \varepsilon l c \tag{16}$$

where
A = absorbance
I = light intensity after penetration
I_0 = light intensity before penetration
ε = absorptivity
l = penetration length
c = concentration

Absorbance is an information can be extracted from the photos. First, a rectangular window is selected from the original image, shown in Figure 3.22. The original photo incorporates the sediment layer at the bottom, the spinner disk at the top, as well as the walls of the beaker. This gives us a better overall impression of the resuspension process. However, for the turbidity analysis, a smaller window of the water column is selected to preserve uniformity. The size of the original picture is 4928 × 3264 pixels. The window selected covers a 1700 × 400 pixels area located at middle left.

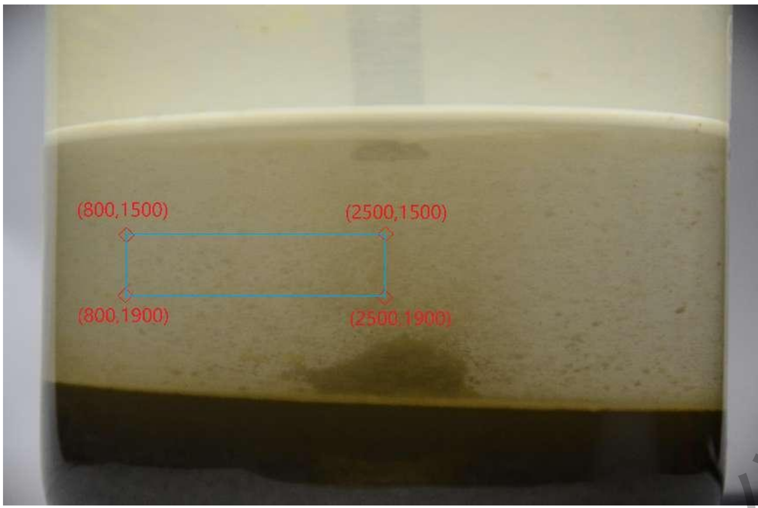

Figure 3.22: The window selected for turbidity analysis.

Then, the cropped images are transformed into gray scale images from RGB colored images using a built-in Matlab function. Every pixel has a gray scale value ranging from 0 to 255, the larger the number, the lighter the color, the higher the light intensity. We average the gray scale values of the pixels to get one single value representing the light intensity of a photo.

For every group of experiment, 5 groups in total, the light intensity of the first image taken at 0 velocity is denoted as I_0. The absorbance of the first image will be 0 in this case. The absorbance of the rest images are calculated by using each of their light intensity as It. An example of this calculation process is shown in Table 8.

Intensity Values	Relative Concentration	$\varepsilon cl = A = -lg(It/I0)$
161.4344664	0	$= -lg(161.4345/161.4345)$
160.4101724	0.002764357	$= -lg(160.4102/161.4345)$
159.5665891	0.005054301	$= -lg(159.5666/161.4345)$

Table 8: A demonstration of calculating relative concentration by comparing light intensity values.

Since concentration is linearly proportional to absorbance, optical path length and absorptivity stay the same throughout every experiment, the values of absorbance is directly used for representing concentration, or turbidity. When relative concentration is mentioned in the following paragraphs, it actually means absorbance, εkl.

3.6.3 Critical Shear Velocity: Experiment Values

Plotting the relative concentrations against the bed shear velocities, we can get the following graphs shown in Figure 3.23.

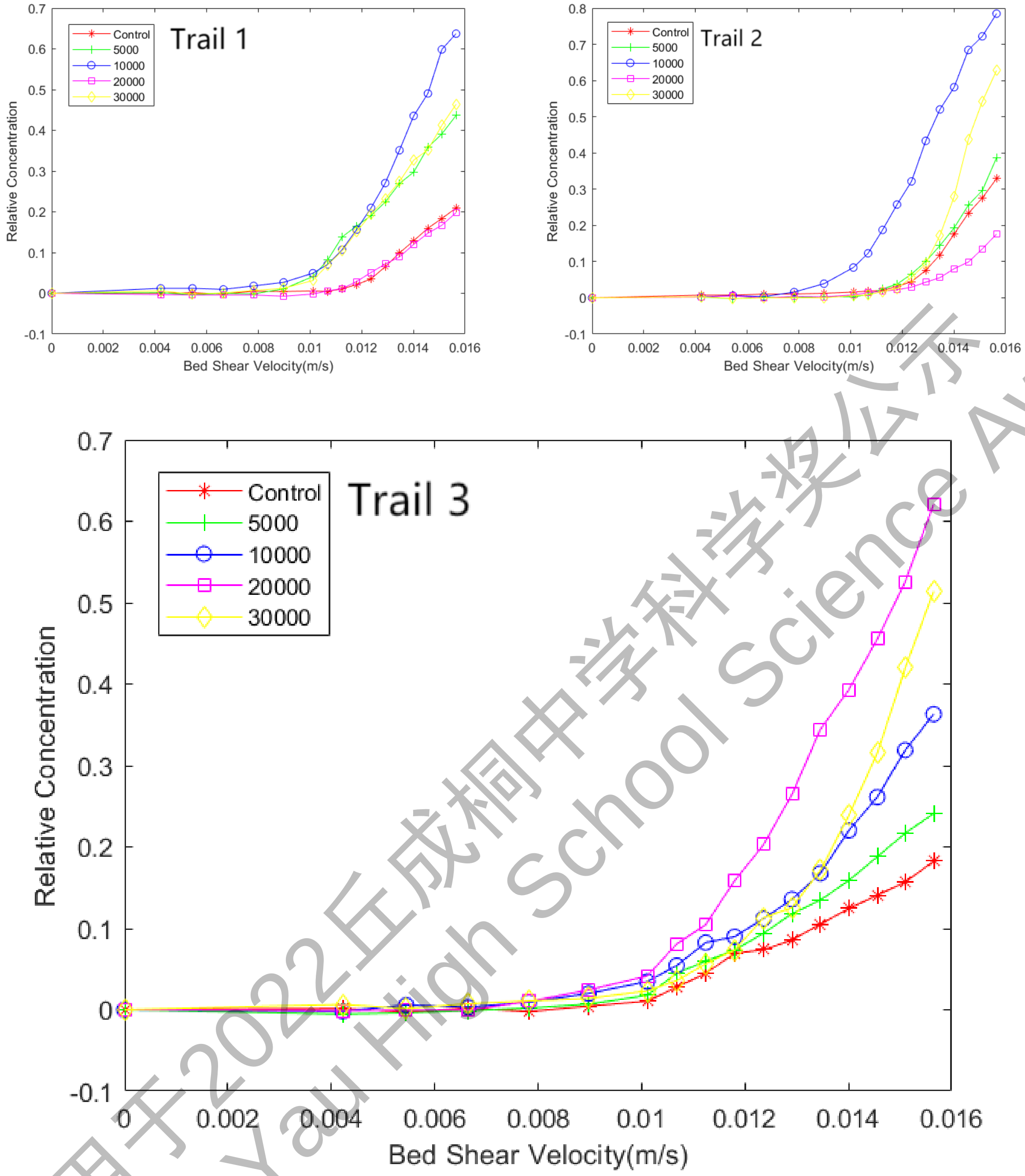

Figure 3.23: The three graphs corresponding to three times of experiments.

What conclusion can we draw from these graphs? First, it has to be admitted that the data across the three repeated experiments show large variability. For example, the purple line representing the group 20000 has fluctuated from the lowest concentration among all groups to the largest. In short, the experiment results are not successful enough to yield strong arguments. Still, the data is worth analyzing to provide us insights and guidance for further experiments. For this study, due to time limitation, no more experiments are done.

1) Height of the Curves: By comparing the height of the curves, we mean comparing the relative concentrations at same bed shear velocities. If we divide the five groups into two broad categories, no microplastics and with microplastics, we can see that the red curve representing no microplastics lies below the other curves, except for one time where the lowest curve is the purple 20000 curve. Therefore, a general impression is that adding microplastics does decrease the resuspension critical velocity as predicted.

2) Resuspension Sequence: We now focus on more detailed information, trying to find a sequence of resuspension between the 5000, 10000, 20000, and 30000 groups. We want to know the value of the critical resuspension shear velocity across the groups. Here, critical resuspension shear velocity is defined as the shear velocity imposed on the sediments when the relative concentration of resuspended particles reach a certain value. By drawing horizontal lines whose height are the desired concentration values and finding the intercepts

of the horizontal lines and the curves, shown in Figure 3.24, we can get lists of critical shear velocities, shown in Table 9:

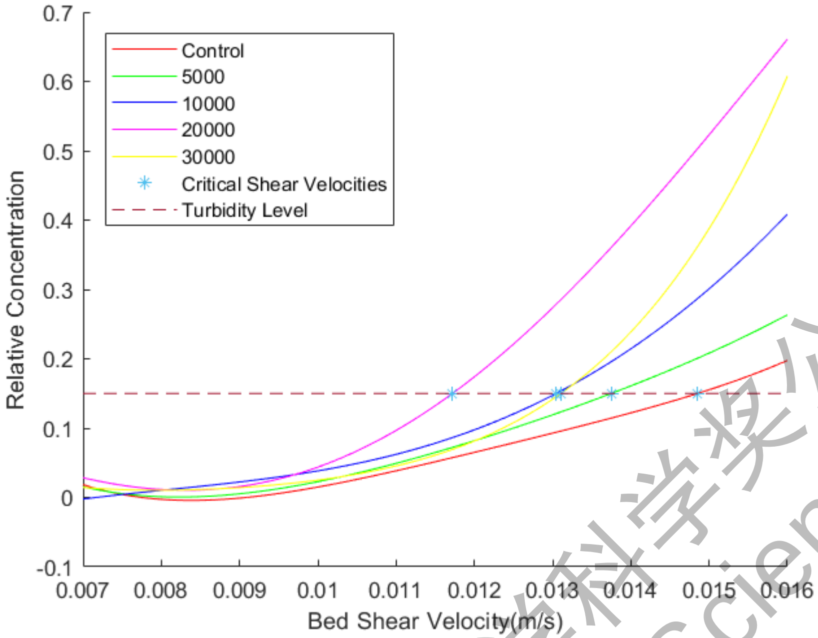

Figure 3.24: An example of finding critical shear velocities: The original discrete data is fitted with a polynomial to generate a continuous curve; The standard of resuspension set at relative concentration = 0.15; a horizontal line is drawn; intercepts are found and their x coordinates are recorded as the critical shear velocities.

Relative Concentration			0.05	0.10	0.15
Critical Resuspension Velocity	**Experiment_1**	control	0.01257	0.01354	0.01440
		5000	0.01004	0.01090	0.01167
		10000	0.01015	0.01115	0.01178
		20000	0.01241	0.01361	0.01466
		30000	0.01029	0.01112	0.01184
	Experiment_2	control	0.01232	0.01315	0.01377
		5000	0.01202	0.01290	0.01355
		10000	0.00947	0.01033	0.01090
		20000	0.01322	0.01453	0.01532
		30000	0.01226	0.01277	0.01316
	Experiment_3	control	0.01144	0.01325	0.01485
		5000	0.01103	0.01250	0.01375
		10000	0.01054	0.01206	0.01305
		20000	0.01015	0.01105	0.01172
		30000	0.01116	0.01237	0.01311

Table 9: Critical shear velocities calculated from the experiments. Three relative concentrations, 0.05, 0.10, and 0.15, are used as standards, when reached, resuspension happens. There are three repeated times of experiments, each consisting five groups, thus for every relative concentration standard, we get fifteen critical shear velocities. The smaller these velocities are, the easier the resuspension.

Now we sort the velocities in ascending order. We label the five groups in each experiment with 1 to 5, from low critical shear velocities to high ones. We get Table 10:

Relative Concentration			0.05	0.10	0.15
Critical Resuspension Velocity	**Experiment_1**	control	5	4	4
		5000	1	1	1
		10000	2	3	2
		20000	4	5	5
		30000	3	2	3
	Experiment_2	control	4	4	4
		5000	2	3	3
		10000	1	1	1
		20000	5	5	5
		30000	3	2	2
	Experiment_3	control	5	5	5
		5000	4	4	3
		10000	2	2	2
		20000	1	1	1
		30000	3	3	4

Table 10: The sequence of resuspension critical shear velocities.

From Table 10 we can see that the sequences are relatively stable within local experiments, but are inconsistent across experiments. It seems that higher concentration of microplastics doesn't necessarily leads to lower resuspension critical shear velocities.

3) Gap Size Between the Curves: By expectation, the curves should be nearly evenly spaced, getting easier to resuspend as the concentration of microplastics increase. However, from the previous data charts, we conclude that this is not true. As shown in Figure 3.25, sometimes, the gap can be large, representing a significant critical velocity change; sometimes, the curves overlap with one another, and the effects of adding more microplastics is blurred.

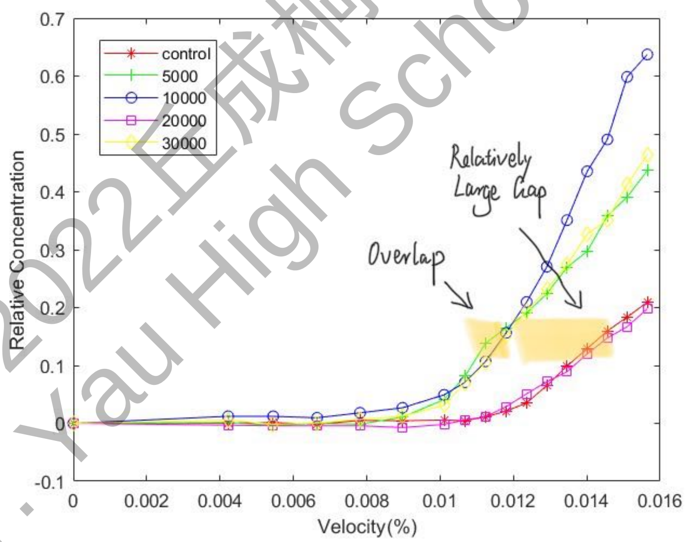

Figure 3.25: A demonstration of velocity gap and overlap.

Compare the data listed in Table 9, we can find the largest velocity gaps are around 0.002 m/s to 0.003 m/s, between the control groups and the groups with microplastics. The critical shear velocities of the control groups are around 0.012 m/s to 0.014 m/s. Combine the two data, we can conclude that at appropriate conditions, the addition of microplastics can decrease the critical shear velocity of resuspension for about 14% to 25% .

So, what might be the causes of the differences between theory predicted results and experimental results? Where does the errors come from? Here are some possible explanations:

1) Time: The three sets of experiments were not done during the same time. The time separation between the experiments is at least two days. During that time, the beakers were kept in dark box to inhibit the growth of microalgae. The initial one-week dark process did not kill all microalgae, because there still needs to be some to help "glue" the aggregates of sand and microplastics. So, during the experiment separation times, the microalgae number may further decrease and influence the results. Except for microalgae, there's also other factors related to time. The temperature changed. The water may still evaporate though the beakers are

covered by plastic films.

2) The Central Bump: When we carefully observe the photos during resuspension experiments, we can see the formation of central bumps, shown in Figure 3.26. These bumps form due to the uneven velocity distribution in cylindrical beakers. The velocity at the middle is lower than that at the periphery. Sometimes, instead of directly resuspend, the particles are dragged to the center of the beaker first. At right conditions, the particles settle down at the center. This means that the velocity at the periphery is larger than its resuspension critical shear velocity, while the velocity at the center is smaller than critical shear velocity. This situation will not occur in rivers, but inevitable in our experiment due to the equipment. We suspect that the central bump has a resisting effect toward the water current and lowers the velocity of water around the bump, adding uncertainty to our experiment. The size of the bump seems relevant to the existence of microplastic-sediment aggregates. When aggregates are present, the bumps are considerably larger. Figure 3.27 illustrates this heterogeneous sediment effect.

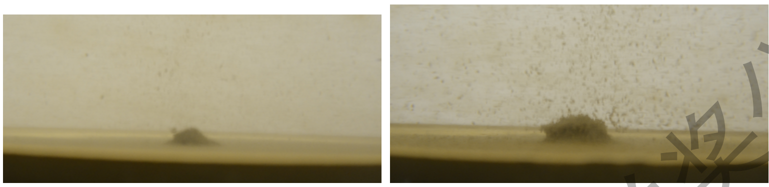

Figure 3.26: Two central bumps: the left from a control group, the right from a group with microplastic concentration of 30000.

2) Heterogeneous Sediment: The resuspension theory mentioned in section 1 is designed for particles with uniform sizes and densities. When making experiment result predictions with measured data of particle diameters and densities, we assumed that all particles are the same. For microplastic-sediment aggregates, we predict their critical resuspension shear velocity to be about 0.0061 m/s, half of 0.012 m/s, the predicted value of pure sand. However, experiment suggest adding microplastics only decrease the critical shear velocity for 14% to 25%. The truth is that not all particles at the surface of the sediment bed are microplastic-sediment aggregates. Adding microplastics only transforms part of the sand particles into aggregates. Therefore, it is not surprising that the decrease isn't as significant as predicted.

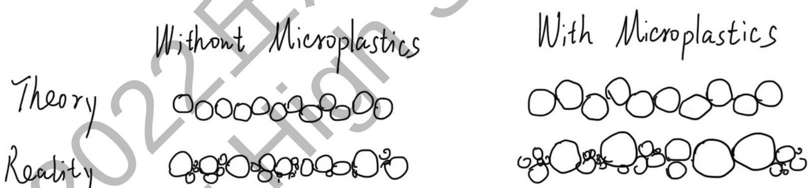

Figure 3.27: The form of the sediment bed: In theory and in reality.

4 CFD Simulation

To further understand the whole process of resuspension under the influence of microplastic presence, the method of CFD, computational fluid dynamics, is applied to aid the experiments. Though the same question being studied, the two methods can provide us different perspectives, each showing their own strengths and weaknesses. Thus, applying both methods simultaneously is beneficial for the integrity and reliability of this study.

The strengths and weaknesses of experimentation:
strengths:

- Fully reflect the real situation, high reliability
- Results are intuitive, easier to interpret

weaknesses:

- Time-consuming and expensive

- Difficult to isolate and control every variable
- Prone to error caused by careless operation
- can only test limited conditions and yield limited data

The strengths and weaknesses of CFD:
strengths:

- Fast and convenient
- Flexible, easy to adjust parameters and repeat
- Less prone to human error
- Cover a broad range of conditions
- Offers more complete data

weaknesses:

- Based on models, not as convincing as experiments
- May deviate from real condition severely due to wrong settings
- Require knowledge and experience about the software

4.1 CFD software: Ansys Fluent

Fluent is a commercial software specialized in computational fluid dynamics. Fluent provides physic models where the user can adjust settings according to the problem studied. The normal procedure of CFD consist three parts: pre-processing, solution, and post-processing. By creating an Ansys Workbench Project, the three steps are achieved one by one. A geometry is designed based on the problem description, then meshing is done to split the computational field into cells. Solution settings are selected, including defining the models, materials, boundary conditions, etc. The calculation is initiated and after its completion, data are collected and analyzed.

4.2 Case Description

Instead of water spinning in a cylindrical beaker, CFD isn't limited by the difficulty of building large water tank and circulatory systems. A situation more analogous to real river flow is simulated. A cross section parallel to the direction of the flow is extracted, shown in Figure 4.1. It is a small area that incorporates part sediment part water.

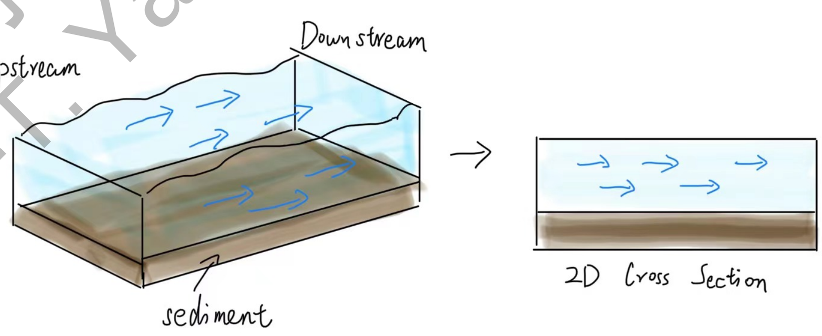

Figure 4.1: A cross section of the river selected for simulation

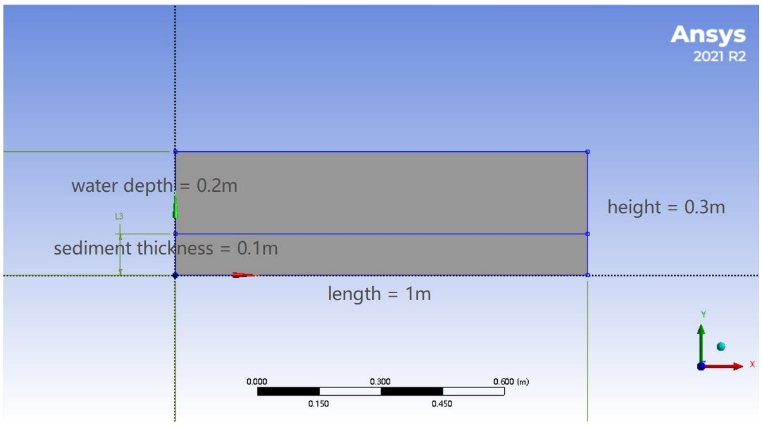

Figure 4.2: Geometry drawn by DesignModeler: A plane of length 1m and height 0.3m is split into the upper water area and the bottom sediment area, each has a depth of 0.2m and 0.1m.

The area adopted has a moderate size - larger than the experiment beaker scale but smaller than the river scale. Such a size is large enough for a general resuspension to occur in natural rivers, while small enough to remain focusing on the local resuspension behavior instead of the whole hydrology of the river. As shown in Figure 4.2, the lower part is filled with sediment, which can be pure sand, also aggregates of microplastic and sand. A small amount of greenhouse gases also exist in the sediment, evenly distributed at a concentration normally observed in rivers. Water flow into the area from left and escape from right at a constant speed. As water flushes in, sediments will experience a shear stress from the water above and resuspend, being carried downstream by the water. Meanwhile, the greenhouse gases in the sediment will be released into the water, or carried away by the water as well. The effect of microplastics aggregating with the sand particles is simplified through adjusting the density and size of the sediment particles according to experiment results. With the addition of microplastics, the density of the particles will decrease while the particle size may increase. Several combinations of densities and sizes are tested. Resuspension rate and greenhouse gas release rate are monitored to reflect the influence of microplastics.

4.3 Solution Settings

4.3.1 Meshing

Mesh is generated and mesh quality is checked. The cells are quadratic, each having a side length of about 1cm. This yields a total cell count of around 3000, shown in Figure 4.3.

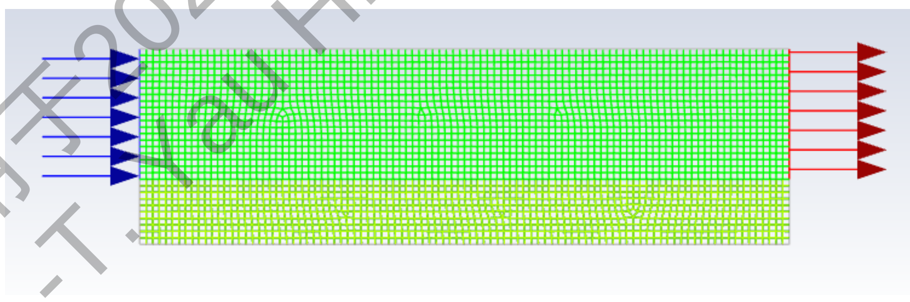

Figure 4.3: The mesh: The two parts, sediment and water are divided into cells; The blue arrows locate the water inlet; The red arrows locate the water outlet.

Fluent is initiated as a 2D case, double precision calculation. Eularian Multiphase Model is turned on to solve the problem, a three phase flow circumstance. The Eularian Model monitor the condition of every cell, specifically, how much matter enter and exit the cells. In this case, which the three phases are water, sediment, and greenhouse gases, the change of the phases in every cell is monitored separately. Combining the information of the three phases of every cell, a whole picture will form.

4.3.2 Material Definition

Liquid water is set as the primary phase. Sand and air are the secondary phases. Sand is granular, having adjustable particle diameter and density. The material is named sand for convenience, but technically, it refers to a mixture of sand and microplastic-sand aggregates.

4.3.3 Phase Interaction

The forces between the phases are defined. Drag force and lift force are considered. Appropriate models are loaded in the software are used to calculate the forces.

4.3.4 Boundary Conditions

The left, right, and bottom of the area is enclosed by walls that are under no-slip condition. The top of the area is a free surface that has zero shear stress. This is a simplification for the water surface of a river, where water meets the air. The interaction between water and the open air isn't the interest of the study, therefore, a zero shear stress setting will suffice. The inlet on the left is a velocity inlet, through which water enters at a constant speed, at 0.2m/s in this case. The outlet on the right is a pressure outlet that all three phases may exit.

4.3.5 Initialization and Calculation

The whole area is first initialized, with water filling the area and more water coming from the inlet. Then the lower part, the sediment area, is initialized, being filled with sand phase and air phase. Because the sediment is mostly sand with tiny amount of greenhouse gas buried in the sediment, the volume fraction of sand phase is set to be 0.999 while air phase 0.001. The sediment area is a stationary bed, meaning the phases all have zero velocity at the beginning. The calculation has 200 time steps, each 0.05s long, generating a simulation of 10s of resuspension process.

4.4 CFD Results

4.4.1 Inputs and Outputs: The change of sediment properties and the effects on resuspension

Inputs: By changing the properties of the sediment particles, the effect of microplastic-sediment aggregation is incorporated into the simulation. Several combinations of density and diameters are trialed.

- Sediment Particle Density(kg/m^3): Three density values are trialed, 1500kg/m^3, 2000kg/m^3, and 2500kg/m^3.
- Sediment Particle Diameter(m): Three diameter values are trialed, 100μm, 200μm, and 300μm.

The three densities and three diameters combine with one another to form nine groups of calculations. They are labeled as group 1 to 9.

density(kg/m^3) / diameter(μm)	100	200	300
1500	group1	group2	group3
2000	group4	group5	group6
2500	group7	group8	group9

Outputs: To assess how microplastics influence sediment resuspension and greenhouse gas release, some quantities are monitored. The value of these quantities across different groups of trials are compared.

- Numerical Data: volume of sand and air: The volume of sand and air remaining in the simulated area is calculated every time step. As water scours the riverbed, sand resuspends. The resuspended sand and released air will exit the simulated area through the outlet. As time proceeds, the sand and air volume remaining in the area will decrease. The remaining volume across each of the nine groups of calculations can be compared to evaluate the resuspension condition. The smaller the volume remaining, the faster the resuspension.
- Animation: Contour of volume fraction of sand phase and air phase: As shown in Figure 4.4, contour shows the distribution of sand and air in the area. Volume fraction means how concentrated is the phase at a location. For example, if a cell is filled by 90% of water and 10% of sand, then water, displayed in red, has a high volume fraction. On the other hand, sand, displayed in blue, has a low volume fraction. Every 10 time steps, a snapshot of the contour is generated. Linking the photos together, we get an animation of the change of the phases relevant to time. An example is shown in Figure 4.5.

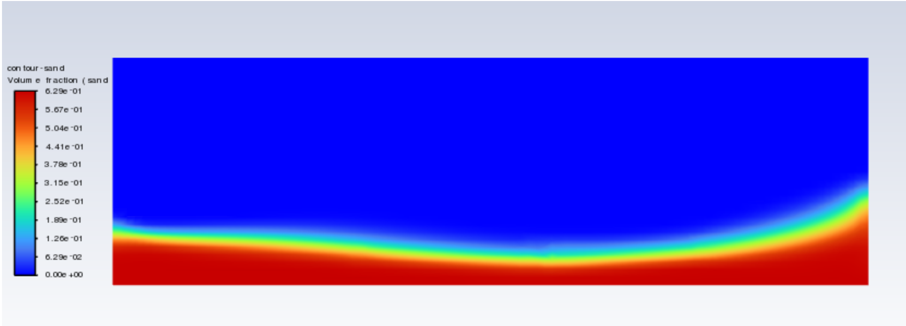

Figure 4.4: An example of the contour of volume fraction of sand phase. The red area at the bottom suggests that most sand is settled at the bottom. The green and yellow color represents the surface where sand and water meet, where resuspension occurs.

- Animation: Contour of sand y-velocity: y-velocity of sand reflects the movement of sand on the direction of weight, perpendicular to the water surface. If sand resuspends, it has positive y-velocity and is displayed in red. Contrarily, if sand settles, it has negative y-velocity and is displayed in blue. The contour of velocity is also recorded as pictures relevant to time.

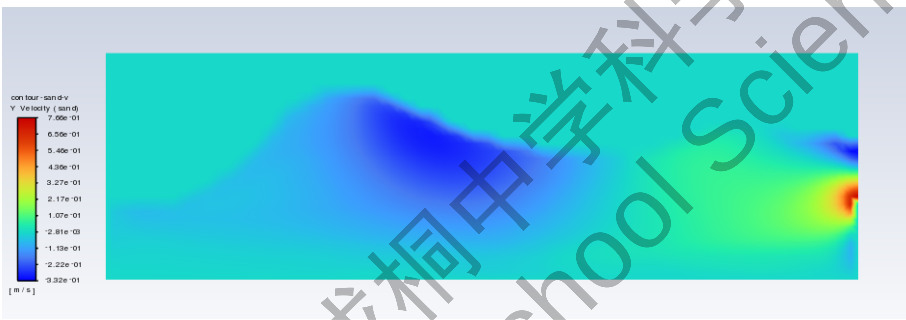

Figure 4.5: An example of the contour of sand y-velocity. Velocity distribution can be read according to the color scale on the left. The greenish blue color means positive velocity. The blue color in the middle may represent the settling of some suspended sediments. The red color at right shows the sand near the outlet being pushed up and exit the outlet.

4.4.2 Data and Analysis

The nine groups of calculations completed within around 4.5 hours, each taking 30 minutes. Output data are collected and processed.

1, The Resuspension of Sand:

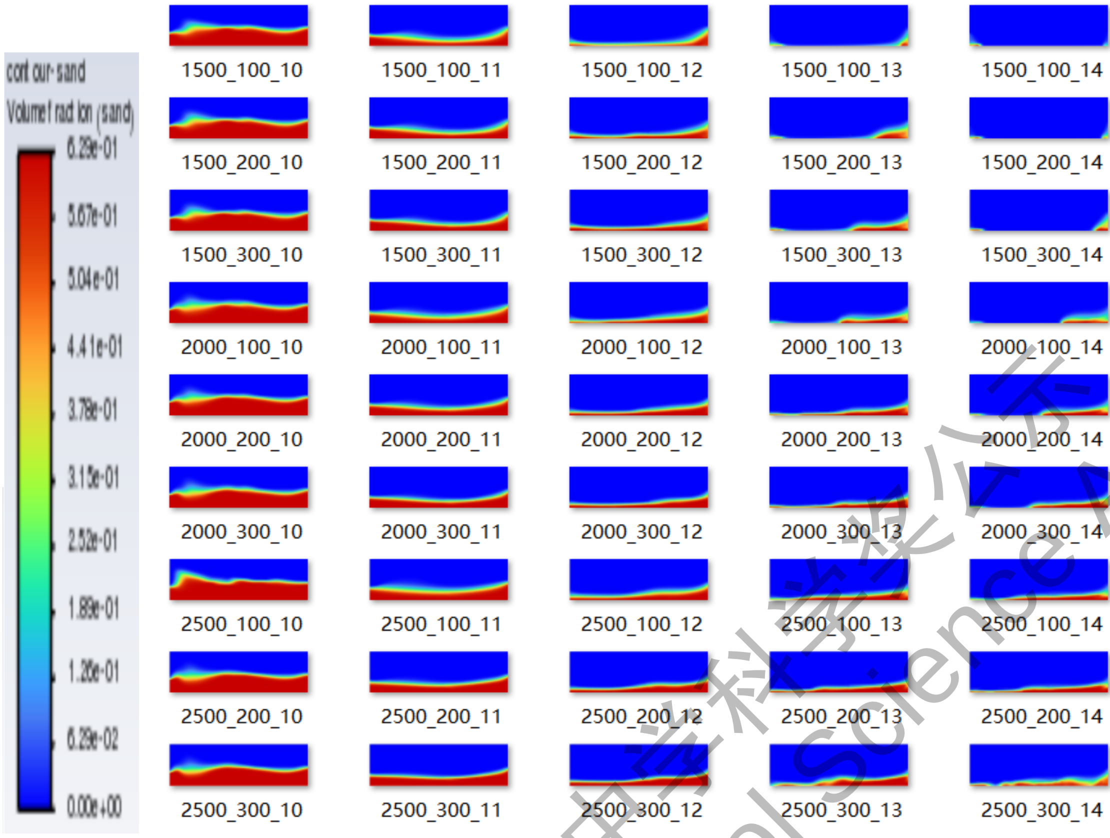

Figure 4.6: The Sand Volume Fraction Contour Across Nine Groups.

Figure 4.6 shows the sand volume fraction contours collected from the simulations. This 5 × 9 matrix of photos can be read from two directions. Each row represents a group of calculation, from 1 to 9. The 5 photos from left to right in each row are the contours of sand during 2s, 4s, 6s, 8s, and 10s. We can see how sand volume decreases as they resuspend and exit the area. The sand moves toward up and right due to drag and lift caused by the water current. The remaining sand are forced into the bottom right corner, forming a flat triangle. This is because the corner is blocked by walls. The outlet is at the upper area, so only the resuspended particles that reach the upper water column may exit. Each column represents the contours of sand across 9 groups after the same time period. By comparing the 9 photos in each column, we can see how fast the eroding is happening in each group. Generally, we find that the groups with a larger diameter and density tend to be less eroded, suggesting their particles resuspends under higher shear stress.

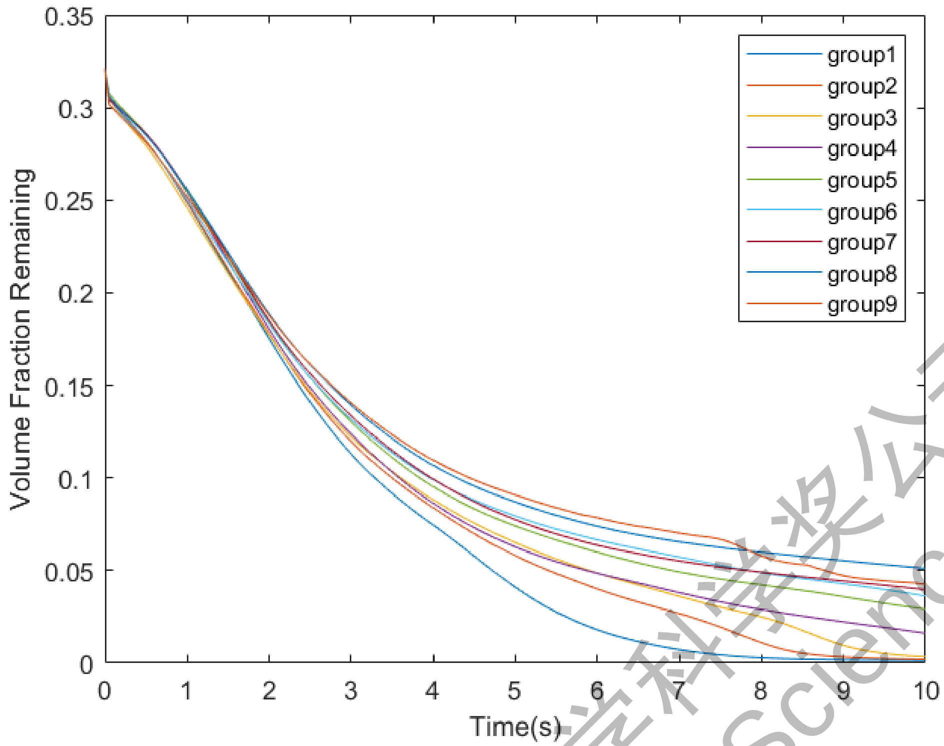

Figure 4.7: Numerical report of sand volume fraction drawn into graph. Each line, consist of 200 data points, represent a group of calculation. The x axis represents time from 0s to 10s. The y axis represents the volume fraction remaining in the area. For example, 0.1 means that the remaining sand fill up 10% of the area.

We can see from Figure 4.7 that all lines are downward sloping, experiencing a steep decrease then a slow decrease. At 0s to 2s, all nine groups decrease at similar rate, then splitting begins. The nine curves show a neat pattern: Curves with smaller diameter and density always lie below the curves with larger diameter and density.

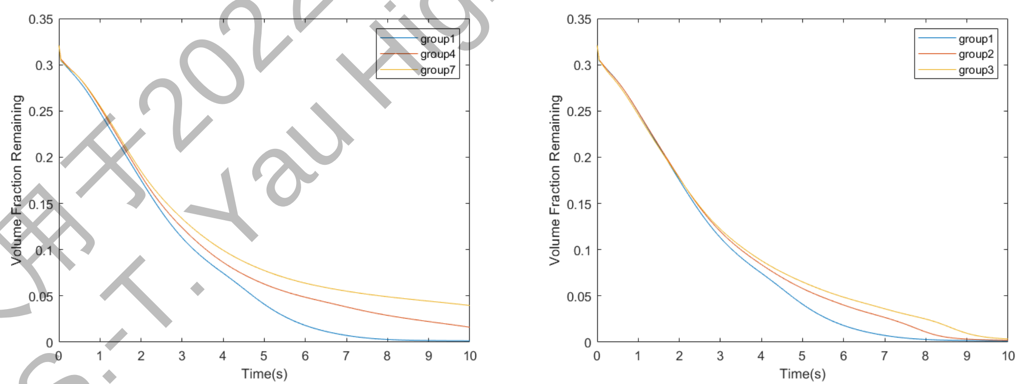

Figure 4.8: Group 1,4,7 are selected to examine the influence of density; Group 1,2,3 are selected to examine the influence of diameter.

In Figure 4.8, we extract out some data from the nine groups in order to have a clearer look. The left graph shows group 1,4,7, all having a diameter of 100 μm but different densities. The right graph shows group 1,2,3, all having a density of 1500 kg/m^3 but different diameters. From the separation of the curves, we can tell that the influence of density is the dominance factor controlling resuspension, which is consistent with our theory.

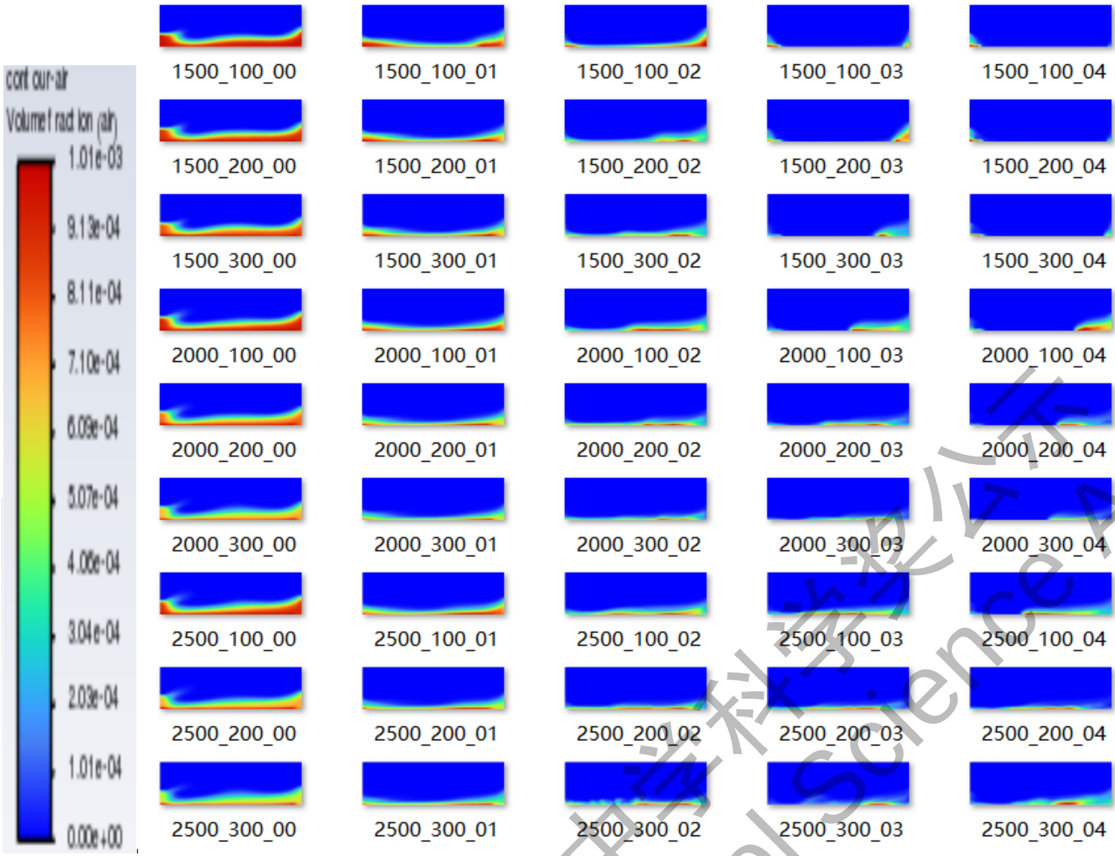

Figure 4.9: The Air Volume Fraction Contour Across Nine Groups

Figure 4.9 shows the change of air volume, representing greenhouse gases release. The pictures can be read the same way as the pictures of sand. The visual effects aren't as vivid as the sand pictures because air loses faster than sand, leaving a very thin layer at the bottom for us to observe. The release of air is influenced by the loss of sand. From the right three columns, we see that there's more chance for air to remain if the volume of sand remaining is larger. This means that when critical shear velocity of the sediments is lowered by the microplastic-sediment aggregates, there will be more sediment resuspension and more greenhouse gas release. Sand acts like a blanket, or a lid, covering the greenhouse gases. Once this cover is opened, the gases escape fast.

In Figure 4.10, we draw the numerical data of air volume fraction remaining into curves as well, and we get similar results as sand.

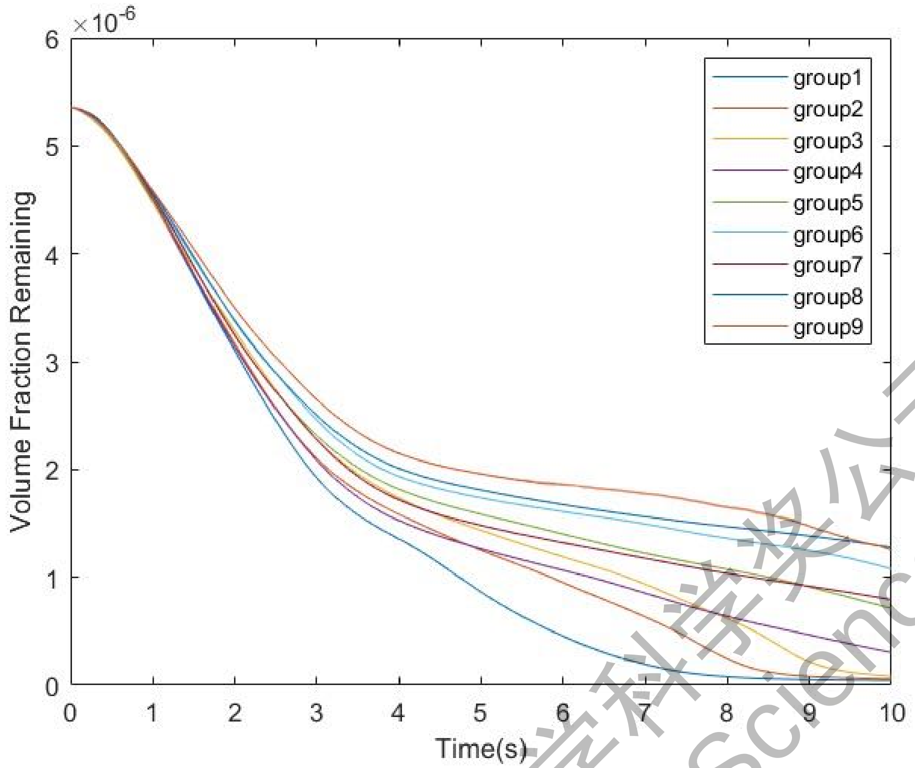

Figure 4.10: Numerical report of air volume fraction drawn into graph.

The air volume decreases the same way as sand, though the initial air volume is set to be 0.1% of the area. Group 7 shows deviation from the pattern, but other groups show the same pattern as sand.

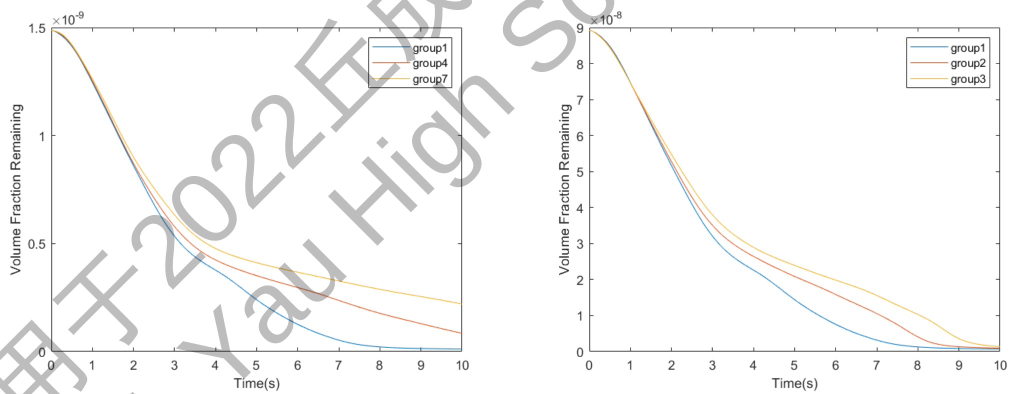

Figure 4.11: Air volume fraction remaining of group 1,4,7 and 1,2,3.

The dominance of density over diameter still can be reflected from the volume change of air, shown in Figure 4.11.

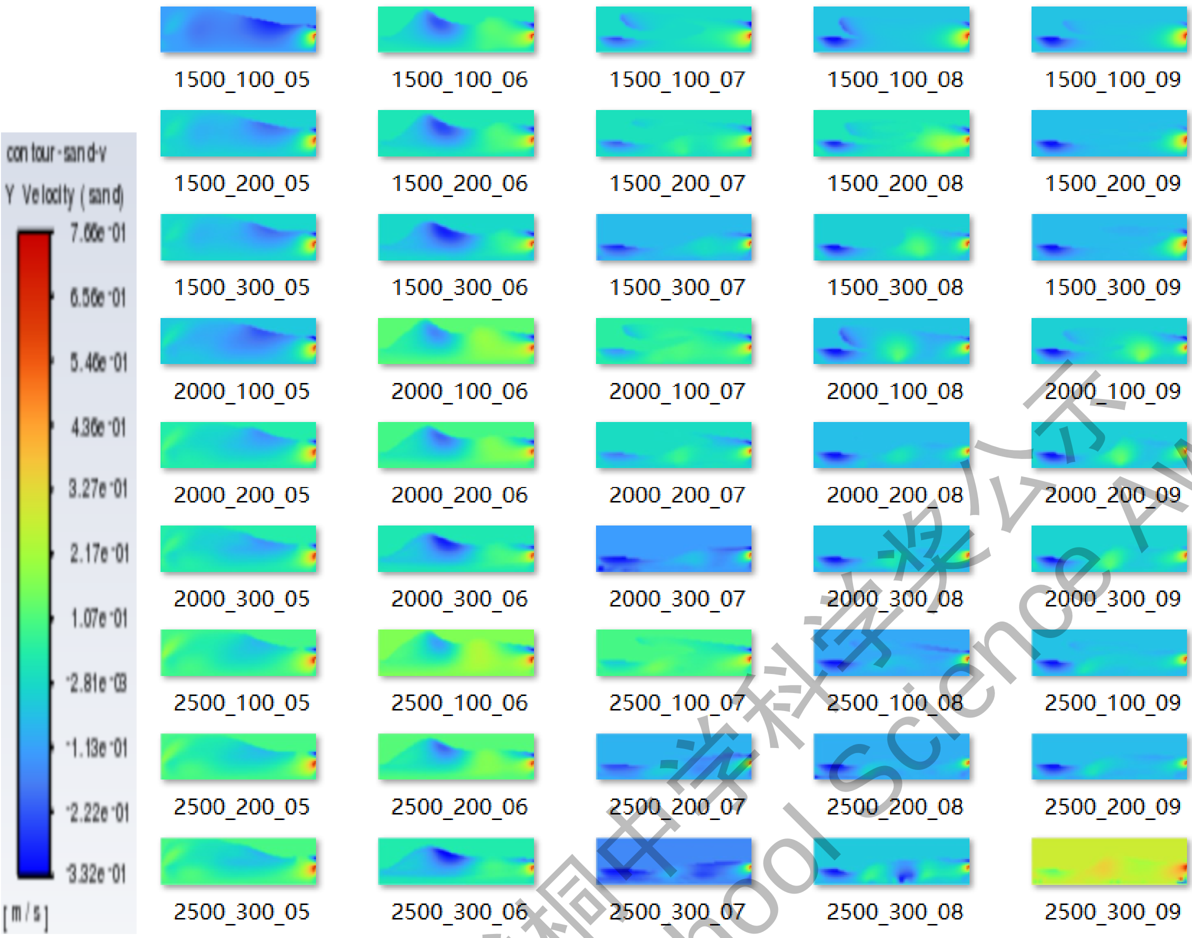

Figure 4.12: The Sand Y-Velocity Contour Across Nine Groups

Figure 4.12 shows the distribution of sand velocity at y direction. The red area at the right wall is caused by the outlet position. Sand near the bottom approach the outlet from below, being pushed upward so they get a high y velocity. The greenish yellow area marks the resuspension zone. We can see how resuspension nearly happens through all bed length, then moves to the right side as sand at the left has been all blown away. The dark blue area marks the settling zone. Some sand particles may have resuspended then settled again. Or, this can happen when the water is eroding the sand, pushing it down before it acquires the right velocity and resuspends.

Combining all data acquired using the CFD method, we again can confirm that by forming low-density aggregates, microplastics indeed promotes the sediment resuspension process. Also, by including the air phase into the simulation, we can see the correlation between sediment resuspension and gas emission: the greenhouse gases buried in the sediments will release quicker if the sediments resuspend.

5 Conclusion

This study started with an hypothesis, that microplastic pollution can change the sediment resuspension conditions in rivers, imposing a potential influence on climate change. Through constructing theories, conducting experiments, and designing CFD simulations, the hypothesis is confirmed: By forming aggregates with river sediments, microplastics effectively lowers the overall particle density and promotes sediment resuspension. Since sediment resuspension is positively linked with greenhouse gas emission, it is reasonable to suspect that microplastic pollution may intensify climate change.

However, there are many questions remaining that require further research. 1) This study only considered spherical microplastics of the same chemical composition and nearly same sizes. What will the effect be if the microplastics are of various shapes, having different properties? 2) Exactly how large will this influence be? The microplastic concentration in our experiment is higher than those measured in rivers in order to yield clearer results and confirm our hypothesis. Does the microplastics in true rivers reach enough concentration to produce significant change to sediment resuspension? If so, how much does the critical shear velocity truly decrease, and how much more greenhouse gases will be released? If not, what will be a dangerous threshold of microplastic pollution? 3) Does the aggregation process in true river resembles the one observed in this experiment?

Just as mentioned in the introduction to this study, environmental issues can be complex. There are numerous factors contributing to environmental issues, making it difficult to identify the role of each single factor. Also, the problem becomes more disturbing when the factors themselves interact with one another. This study is just a small attempt in understanding the relationship between three environmental events: microplastic pollution, sediment resuspension, and climate change. The goal of the study is not to build a perfect theory that explains those problems with one hundred percent certainty. There is still much work to be done. The goal of the study will be reached if the study calls people's attention to the complexity of environmental problems and the urgency of solving them. Acknowledging that human activities, including but not limited to the use of plastics, does pose a threat to the environment we live in, is the first step in truly addressing environmental issues.

References

[1] Alimi, O., Farner Budarz, J., Hernandez, L. and Tufenkji, N., 2018. Microplastics and Nanoplastics in Aquatic Environments: Aggregation, Deposition, and Enhanced Contaminant Transport. Environmental Science amp; Technology, 52(4), pp.1704-1724.

[2] Bejestan, M. and Nouroozpou, S., 2007. Use of Image Processing Technique to Estimate Sediment Concentration. Journal of Applied Sciences, 7(20), pp.3096-3100.

[3] Garcia, M., P. E., Ph. D. and Marcelo Garcia., 2008. Sedimentation Engineering: Processes, Measurements, Modeling, and Practice (ASCE Manuals and Reports on Engineering Practice). American Society of Civil Engineers / ASCE.

[4] Lagarde, F., Olivier, O., Zanella, M., Daniel, P., Hiard, S. and Caruso, A., 2022. Microplastic interactions with freshwater microalgae: Hetero-aggregation and changes in plastic density appear strongly dependent on polymer type.

[5] Law of the wall - Wikipedia. (2022). Retrieved 4 September 2022, from https://en.wikipedia.org/wiki/Law_of_the_wall

[6] Möhlenkamp, P., Purser, A. and Thomsen, L., 2018. Plastic microbeads from cosmetic products: an experimental study of their hydrodynamic behaviour, vertical transport and resuspension in phytoplankton and sediment aggregates. Elementa: Science of the Anthropocene, 6.

[7] Shen, M., Huang, W., Chen, M., Song, B., Zeng, G. and Zhang, Y., 2020. (Micro)plastic crisis: Un-ignorable contribution to global greenhouse gas emissions and climate change. Journal of Cleaner Production, 254, p.120138.

[8] Shields, A., Anwendung der Ahnlichkeitsmechanik und der Turbulenzfor.schung auf die Geschiebebewegung, Mitt, der Preuss. Versuchsanst. fur Wasserbau und Schiffbau, Heft 26, Berlin, Germany 1936.

[9] Stokes' law - Wikipedia. (2022). Retrieved 4 September 2022, from https://en.wikipedia.org/wiki/Stokes%27_law

[10] van Rijn, L., 1984. Sediment Transport, Part I: Bed Load Transport. Journal of Hydraulic Engineering, 110(10), pp.1431-1456.

[11] Wiberg, P. and Smith, J., 1987. Calculations of the critical shear stress for motion of uniform and heterogeneous sediments. Water Resources Research, 23(8), pp.1471-1480.

[12] Zhang, Y., Liang, J., Zeng, G., Tang, W., Lu, Y., Luo, Y., Xing, W., Tang, N., Ye, S., Li, X. and Huang, W., 2020. How climate change and eutrophication interact with microplastic pollution and sediment resuspension in shallow lakes: A review. Science of The Total Environment, 705, p.135979.

Acknowledgements

First of all, I want to express my gratitude to all the teachers who guided me. I first learned about Yau Award from Dr.Zheng Zijie and Dr.Fan shuang from my school, who helped me to discover a new path to approach the subject of physics: through doing scientific research and applying physics to real life problems. When I was deciding my research topic, Dr.Zhong Guohu listened to my concerns and doubts, and gave me advice that are thought provoking. During the experiments, Dr.Xiao and me overcame lots of difficulties together. Instead of telling me the correct answers, Dr.Xiao offered me hints and methods. His guidance helped me to learn from trial and error, making this research an unforgettable adventure and unique experience.

In addition, the supports from my family also provided me with strength. All experiments of this research were done at home, under limited experiment conditions. During these experiments, my parents paid close attention to my work. They even joined me as 'experiment assistants'. Whether it is dad helping me digging sand, or mom 'tolerating' me lining the beakers on the balcony, the supports from my family always make me touched.

Finally, I would also like to thank myself for being principled. The hardest part of this research was the experiments. The data we got weren't satisfying. No clear pattern was identified. There was a period of time when I thought of giving up, using only parts of the data as my results. Yet I realize that would greatly damage the academic honesty of the research, and I chose honesty. I believe that the damage caused by dishonesty is much greater than a few unsuccessful experiments.

In this paragraph, I'd like to talk about the inspirations of my research topic. Though the topic of my research seems grand, it actually started with small things that I've noticed in my life. My hometown is a small village located in the mountains of western Hunan. Over the course of two generations, the village experienced significant changes. Father recalled children swimming and harvesting fish from the rivers when he was young. Yet several years before, the rivers were severely polluted, treated as garbage dumps. You'd see plastic bags being flushed down the rivers during rainfalls. Luckily the situation is improving recently as the government began collecting the garbage with trucks. Other inspirations to choose this topic come from reading and news. When I read about an article on microplastics, I was shocked by how we produce them and use them recklessly (adding microplastics to cosmetic products). I am also shocked by the extreme heat this summer. Many places in China reported temperatures above forty degrees Celsius. The red alarm for high temperature nearly becomes a norm this summer. Will we take these small things as signs or will we continue ignoring them?

A Appendix: Experiment Raw Data

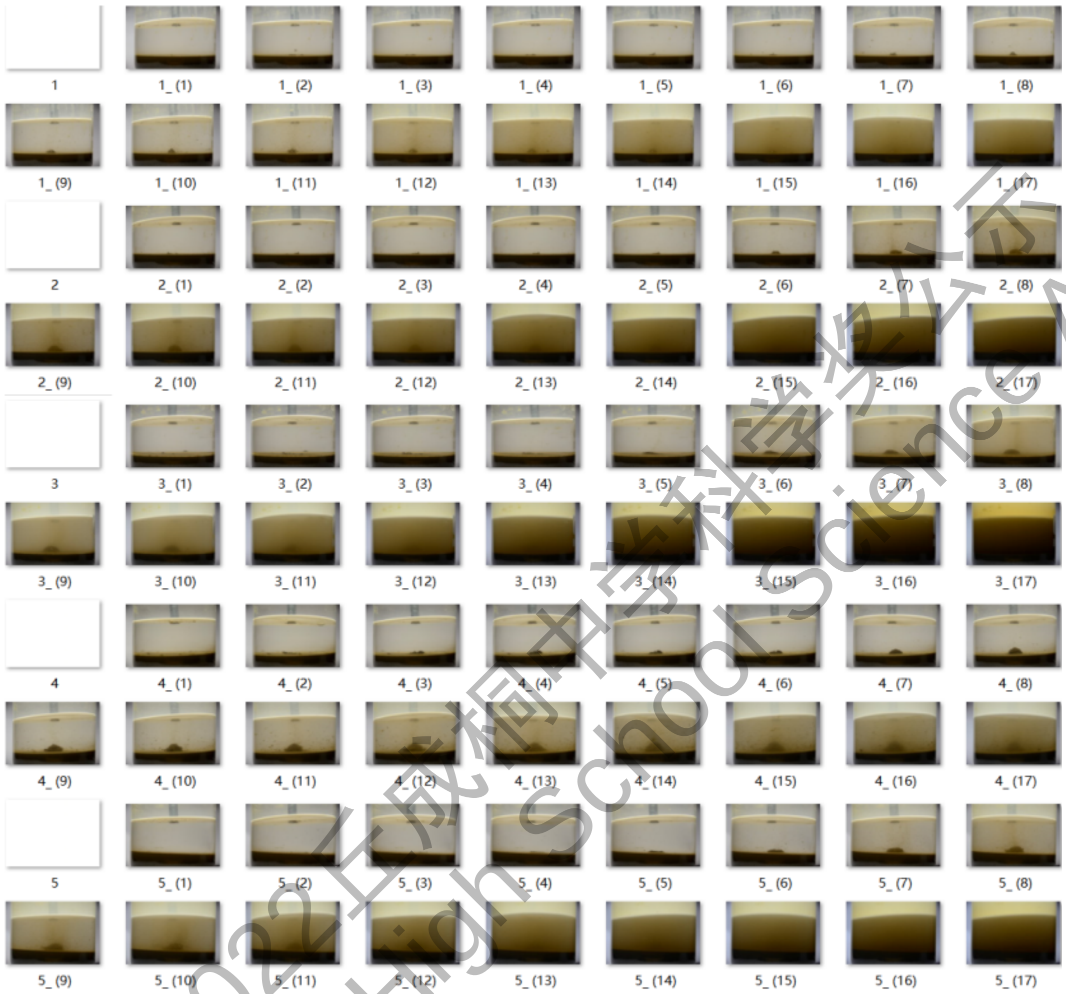

Figure A.1: Photos from the first time of experiment.

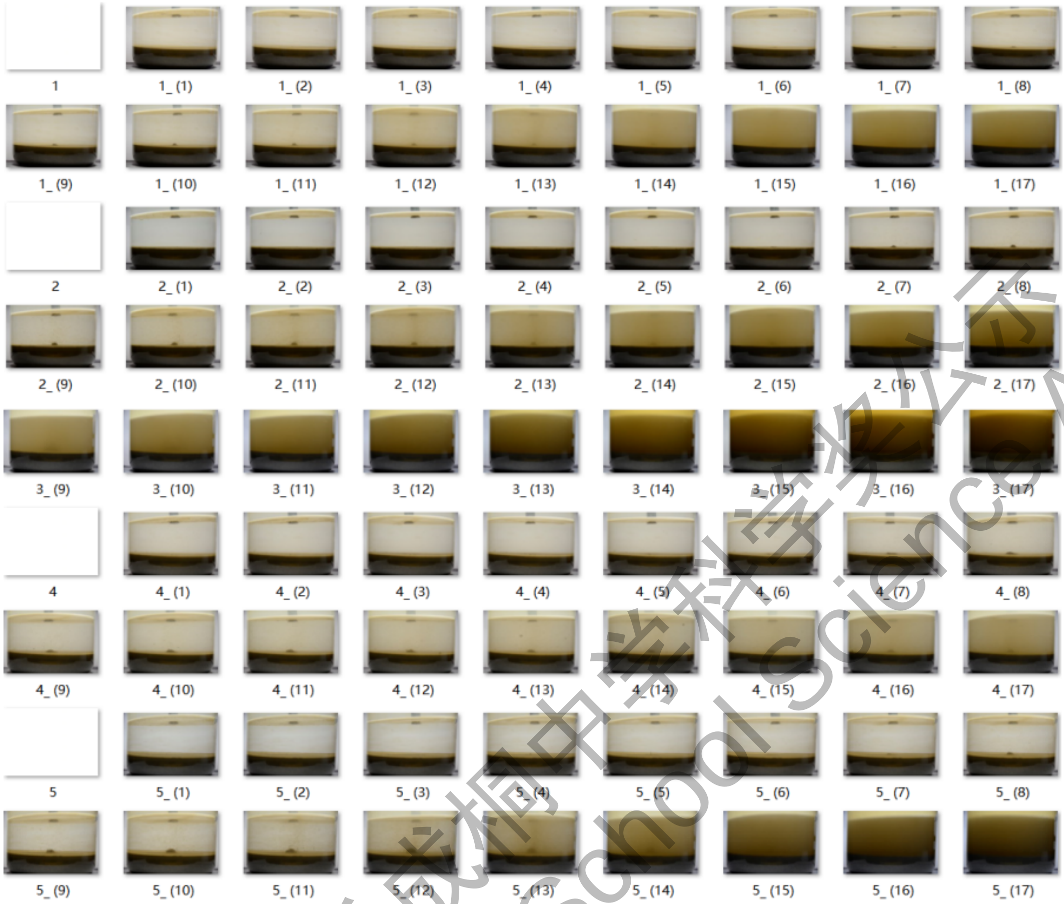

Figure A.2: Photos from the second time of experiment.

Figure A.3: Photos from the third time of experiment.

B Appendix: Timeline

4.1-5.5: Decide the research topic
5.1-5.11: Read relevant research articles
5.5-5.10: Decide approaching the problem from three perspectives: theory,experiment, CFD
5.20-5.25: Prepare experiment materials and equipment
5.31-7.2: Wait for the microplastics to form aggregates; Refine the experiment plan;Get familiar with CFD software; Study the basic concepts of fluid dynamics relevant to the research
7.2-7.5: Preparatory measurements: density and diameter of the particles
7.7: The first experiment conducted
7.14: Experiment repeated
7.30: The third time of experiment
8.1-8.15: Understand the Shields diagram; Analyze the experiment results
8.3-8.10: Design the CFD simulation; Write the CFD section
8.9-8.10: Write the Theory section
8.15-8.20: Write the Experiment section
8.19: First draft finished
8.20-9.15: Final draft